STUDIES IN LOAD-FREQUENCY AND SYNCHRONOUS MACHINE CONTROL

PART A Simulation of a Hydro-Electric Governor System

PART B Modal Control of a Power System

A thesis submitted
in partial fulfilment of the requirements
for the Degree of
MASTER OF TECHNOLOGY

by

INDLA VENKATA RAMANA

to the

Department of Electrical Engineering
Indian Institute of Technology
Kanpur

January 1974

V
'6

I.I.T. KANPUR
CENTRAL LIBRARY
Acc. No. A28387

11 MAR 1974

V
JUNE '76

EE-1974-M-RAM-STU

POST GRADUATE OFFICE
Submitted on 14.1.14.

CERTIFICATE

Certified that this work on 'Studies in Load-Frequency and Synchronous Machine Control' has been carried out under our supervision and that this has not been submitted elsewhere for a degree.

Dr. M.A. Pai
Professor in Elec.Engg.
IIT/Kanpur

Dr. S. S. Prabhu
Asst. Professor in Elec.Engg.
IIT/Kanpur

POST GRADUATE OFFICE
22.1.14

ACKNOWLEDGEMENTS

The author wishes to express his deep sense of gratitude to Prof. M.A. Pai and Prof. S.S. Prabhu for suggesting the problems and for their constant encouragement and stimulating discussions through out this thesis work.

The author also wishes to thank M/s B.H.E.L., Bhopal for providing financial support for the first part of the thesis work, for whom the said research has been carried out.

Finally the author's thanks are due to the authorities of Indian Institute of Technology, Kanpur for providing the computer facilities in connection with the research and his thanks are also due to Mr. K.N. Tewari for his excellent job of typing and to Mr. J.C. Verma for his excellent job of drawing the figures.

TABLE OF CONTENTS
(Part A)

TABLE OF CONTENTS

(Part B)

LIST OF SYMBOLS
(Part A)

P_o - rated power

H - instantaneous value of head

H_o - rated value of head

Z - $\frac{(H-H_o)}{H_o}$ relative head deviation

Q - instantaneous value of turbine discharge

Q_1 - $Q/\sqrt{H}$ unit quantity

Q_r - turbine discharge at gate Y_r and rated speed and head

Q_o - rated value of turbine discharge

q - Q/Q_o relative value of discharge

q_1 - $q/\sqrt{1+Z}$ relative unit quantity

q_{1r} - relative unit quantity corresponding to discharge Q_r

M - instantaneous value of turbine torque

M_1 - M/H unit torque

M_r - turbine torque at gate Y_r and rated speed and head

M_o - rated value of turbine torque

m - M/M_o relative value of torque

m_1 - $m/(1+Z)$ relative unit torque

m_{1r} - relative unit torque corresponding to torque M_r

N - instantaneous value of speed

N_1 - $N/\sqrt{H}$ unit speed

N_o - rated speed of turbine

n - $\frac{N-N_o}{N_o}$ relative speed deviation

n_1 - $(1+n)/\sqrt{1+Z}$ relative unit speed

N_r - extrapolated runaway speed at gate Y_r and rated head; point at which tangent to unit torque unit speed curve intersects the unit speed axis

N_s - $\frac{N_o P_o^{\frac{1}{2}}}{H_o^{5/4}}$ specific speed

R - $(N_r-N_o)/N_o$ relative speed deviation at runaway speed and rated head; also relative unit speed deviation at runaway

T_m - machine time constant; unit acceleration constant in secs.

T_w - pipeline time constant; water inertia time at rated discharge and head in secs.

T_d - characteristic dashpot delay time, secs.

b_t - temporary speed droop

b_p - permanent speed droop

e_t - coefficient of self-regulation of the turbine

e_g - coefficient of self-regulation of the load

e_n - e_t-e_g coefficient of self-regulation of the system

Y - servomotor position measured from the fully closed position

Y_m - maximum value of servostroke

s - Y/Y_m relative value of servomotor opening

Y_r - arbitrary reference position of the servomotor

ε - $(Y-Y_r)/Y_m$ servomotor stroke deviation

α - effective relative gate

β - slope of the tangent of the RUQ versus RUS characteristic at the operating point

γ - $\frac{\Delta\alpha}{\Delta_j s}$ mean slope of the unit quantity - relative gate and unit torque - relative gate characteristics at reference position of the servomotor

δ - $\frac{b_t}{\gamma}$ effective value of temporary droop

η - efficiency

e_i —[a]— $e_o = -\int (ae_i + I.C)dt$ Integrator symbol

I.C.

e_i —[a]— $e_o = -ae_i$ Amplifier symbol

e_i —[a]— $e_o = ae_i$ Gain symbol

e_1 —(+, −)— $e_1 - e_2$ Summing junction symbol

(e_2)

e_i —[G(s)]— e_o Block schematic of transfer function

LIST OF FIGURES

(Part A)

LIST OF TABLES

(Part A)

LIST OF SYMBOLS
(Part B)

Control Theory

A - (nxn) matrix of the system without control

A_1 - (nxn) matrix of the closed-loop system

B - (nxr) matrix of control

J - cost functional

K - Riccati matrix (gain matrix)

Q, R - Positive definite matrices

$\underline{x}$ - n-vector of state variables

$\underline{u}$ - r-vector of control variables

u_1, u_2 - control signals

u_v, u_g - control signals (see eqn.(D.10))

$\underline{b}$ - column vector of matrix B

$\underline{G}$ - n-vector of feedback gains

Λ - diagonal matrix of eigenvalues

$\underline{U}$ - eigenvector of matrix A

$\underline{V}$ - eigenvector of matrix A'

$\underline{W}$ - eigenvector of closed-loop system matrix A_1

λ - eigenvalue of open-loop system

ρ - eigenvalue of closed-loop system

η - approximate measurement of mode

k - controller feedback loop gain

p - scalar quantity (see eqn.(B.8))

ζ - damping ratio

w_n - undamped natural frequency

$'$ - transpose of a matrix or a vector.

System parameters and variables (all in per unit otherwise stated)

B - transmission line susceptance

x - transmission line reactance

D - damping coefficient of machine

H - inertia constant

x_d - synchronous reactance d-axis

x_d' - transient reactance d-axis

x_q - synchronous reactance q-axis

X_d, X_q, X_d' - see eqn.(D.11)

τ_{do}' - open-circuit time constant of the field

τ_e - exciter time constant

τ_s - voltage control feedback loop time constant

τ_g - gate time constant

τ_a - governor actuator time constant

τ_w - water time constant

μ_e - exciter gain

μ_s - voltage control feedback loop gain

μ_a - governor actuator gain

σ - permanent droop

P_i - mechanical power input

P_e - power of the electro-mechanical energy conversion

P - generator power output

Q - generator reactive power output

V_o - infinite bus voltage, assumed constant

V_t - generator terminal voltage

V_d - d-component of V_t

V_q - q-component of V_t

V_f - field voltage

ψ_f - field flux linkage

δ - torque angle (radians)

w_o - synchronous speed (377 rad./sec.)

w - speed (rad./sec.)

n - speed (rad./sec.), after time scaling

g - gate opening

g_f - governor feedback loop signal

h - water head

β - time scaling factor

τ - scaled time (sec.)

o - initial value of a variable (subscript)

$'$ - deviation from the initial value of a variable.

LIST OF FIGURES
(Part B)

LIST OF TABLES
(Part B)

SYNOPSIS
(Part A)

In this part of the work, the analog simulation of a hydro-electric governor system is presented, taking into account the true turbine characteristics. Effect of parameter variations such as speed dependence of flow, gate variations are studied both on stability and transient response of the system, and optimum adjustment of governor parameters is indicated. Comparison is made between the different models of the system including the classical model.

SYNOPSIS

(Part B)

In this part of the work the modal control approach is employed to improve the transient response of a power system by shifting the dominant eigenvalues of the uncontrolled system farther towards the left in the complex plane, using complete as well as incomplete state feedback. A sector criterion is used for preassigning the new locations of the eigenvalues and selection of appropriate control inputs for shifting is indicated. The advantages of the modal control approach over the frequently used approach using optimal linear state regulator formulation are discussed.

PART A

SIMULATION OF HYDRO-ELECTRIC GOVERNOR SYSTEM

CHAPTER 1

INTRODUCTION

The study of optimum adjustment of governor parameters of a hydro-electric system, hitherto, have used in most cases an approximate model for the turbine part of the power system. The true turbine characteristics were completely ignored, which as shown by Goldwag [1] have significant effect on the stability and transient response of the system. Step by step methods are available, which take into consideration the true turbine characteristics and give solutions with greater accuracy. But these methods are too involved when dealing with problems with small excursions of gate or problems of stability. Hence a labour saving method, representing at the same time the turbine more accurately, is needed to have better results.

A more accurate linearized model of water turbine has been developed by Goldwag [1] and theoretical investigation (Appendix B) of the problem of stability for all types of machines at all gate openings has been made by him. He has also discussed the effect of turbine characteristics on the optimum setting of governor parameters based on two criteria. According to him, if we draw the limit of stability curve, and if we denote

the point of critical damping and further draw the curve corresponding to the product $b_t T_d$, (temporary droop and dash pot time constant product), obtainable at the point of critical damping, then the possible region of operation would be between the two curves. The former curve does not represent a preferred setting of governor parameters and the latter critical damping curve may or may not represent a suitable setting depending on the value of $(b_t T_d)_{cr}$. In any case, a setting of governor parameters with $b_t T_d$ value less than or equal to $(b_t T_d)_{cr}$ is normally preferred.

In a recent paper Pai and Ganesan [2] have discussed the optimum adjustment of governor setting using parameter plane technique. They have used only an approximate model for turbine. It will be shown in the Chapter 2 that their model which is referred as the classical model is a special case of that of Goldwag. Further more compatibility between these models is established via the well known block diagram language of the control engineer.

Another accurate linearized model of the turbine is given by Ramey and Skooglund [3]. This suffers from the defect that certain coefficients are to be determined experimentally for the particular installation under consideration. In Chapter 2 a

comparison is made between this model and that given by Goldwag.

In Chapter 3 analog simulation of the hydro-electric governor system, as given by Goldwag is carried out and the theoretical results of stability as predicted by Goldwag are verified. In addition the effect of self-regulation of the system, which was neglected by Goldwag in his theoretical investigation, has been studied and the results verify with those given by Pai and Ganesan [2].

CHAPTER 2

HYDRO-ELECTRIC GOVERNOR SYSTEM MODEL

2.1 Mathematical Model taking into account True Turbine Characteristics

The basic differential equations of the water turbine system as such can be derived from the information of the turbine characteristics like relative unit quantity (RUT) versus relative unit speed (RUS), relative unit torque (RUT) versus RUS and relative servo opening (RSO) versus RUQ and RUT. These characteristics are available either as experimental data or can be derived from Mussel Curves [1,4], usually provided. The basis for the derivation of the turbine system differential equations is that the above mentioned characteristics can very closely be represented by straightline tangents at the point corresponding to the unit speed around which an excursion of gate or the stability is to be investigated. As a result certain new parameters are introduced (Figures A.3, A.4, A.5), which are

i) β - the slope of RUQ versus RUS characteristic

ii) e_t - the slope of RUT versus RUS characteristic

iii) α - the relative effective gate, which is defined by the equation

$$\alpha = g + \gamma s \qquad (1)$$

where γ is the slope of effective gate versus RSO characteristic (Figure A.5).

The detailed derivation of the turbine system dynamic equations is given in Appendix A. The two basic differential equations derived for the turbine system are as follows

$$-\frac{Z}{T_w} = \frac{dq}{dt} = \gamma \frac{d(\Delta s)}{dt} + \frac{(\alpha - \beta)}{2} \frac{dZ}{dt} + \beta \frac{dn}{dt} \qquad (2)$$

and

$$T_m \frac{dn}{dt} = \gamma \Delta s + \frac{(3\alpha - \beta)}{2} Z - [(\alpha - \beta) - e_g]n \qquad (3)$$

subject to the assumptions that the slope of the RUQ versus RUS characteristic does not vary significantly with gate and the bulk water hammer represents adequately the pressure changes following the variations of flow.

Since the main interest is to show the effect of the true turbine characteristics, the most basic form of transfer function for the governor is assumed and is given by

$$\Delta s = -\frac{(1 + T_d S)n}{b_t T_d S} \qquad (4)$$

Equations (2), (3) and (4) represent mathematically the isolated hydro-electric system under consideration.

2.2 Block Diagram Representation of the System

The mathematical model of the system given by eqns.(2), (3) and (4) can conveniently be represented by means of a block diagram, well known to control engineers, the development of which follows.

The governor transfer function given by eqn.(4) can be represented by a block diagram given in Figure 1a. The corresponding state variable diagram is given in Figure 1b.

The turbine system eqns.(2) and (3) can be represented by the two block diagrams given in Figures 2a and 3a. The corresponding state variable diagrams are given in Figures 2b and 3b.

Combining the blocks given in Figures 1a, 2a and 3a and doing certain simple manipulations, a composite block diagram given in Figure 4a is obtained, which represents the hydro-electric governor system. The corresponding state variable diagram is given in Figure 4b. In the Figures 4a and 4b, δ is defined as effective temporary droop, which is given by

$$\delta = \frac{b_t}{\gamma} \qquad (5)$$

and ΔL is a step load change.

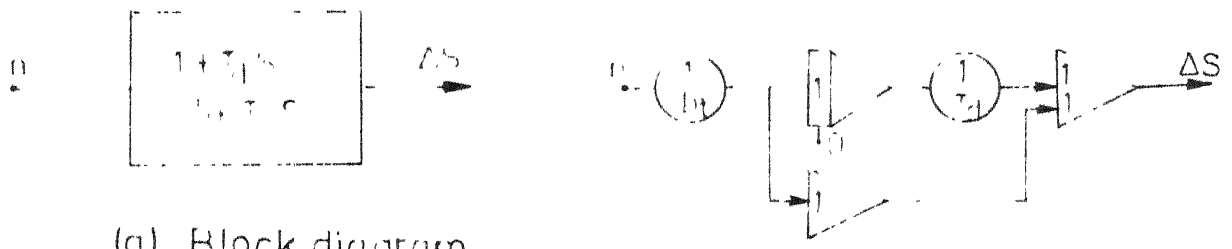

(a) Block diagram (b) State variable diagram

FIG.1 GOVERNOR REPRESENTATION

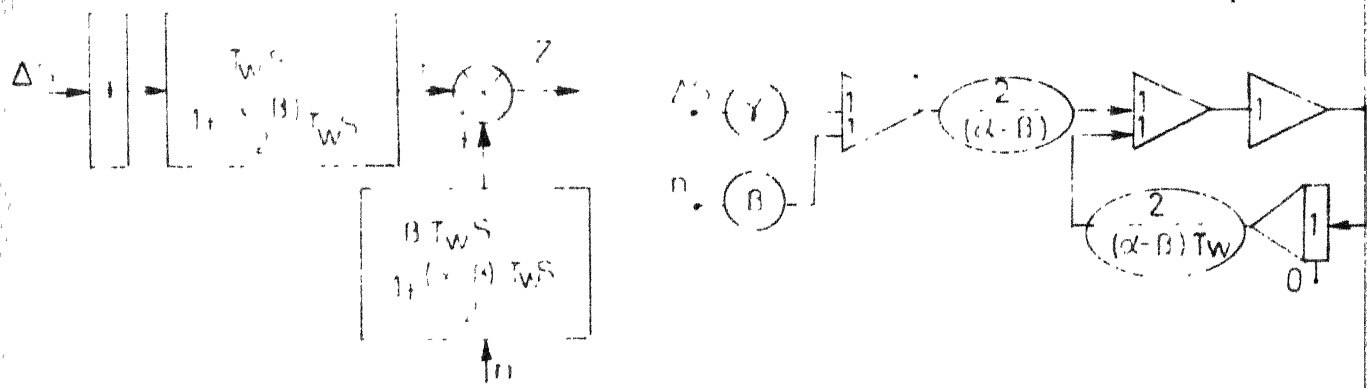

(a) Block diagram (b) State variable diagram

FIG.2 TURBINE REPRESENTATION

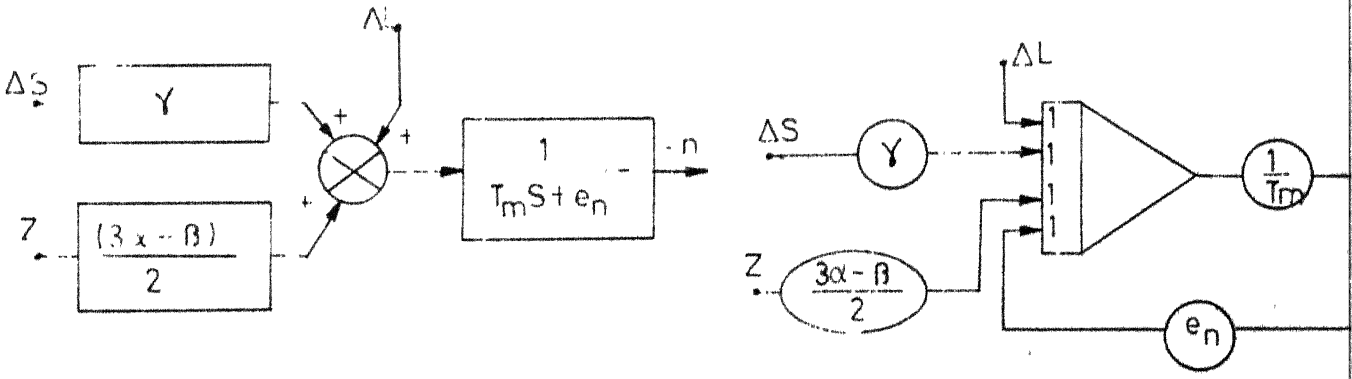

(a) Block diagram (b) State variable diagram

FIG.3 SYSTEM REPRESENTATION

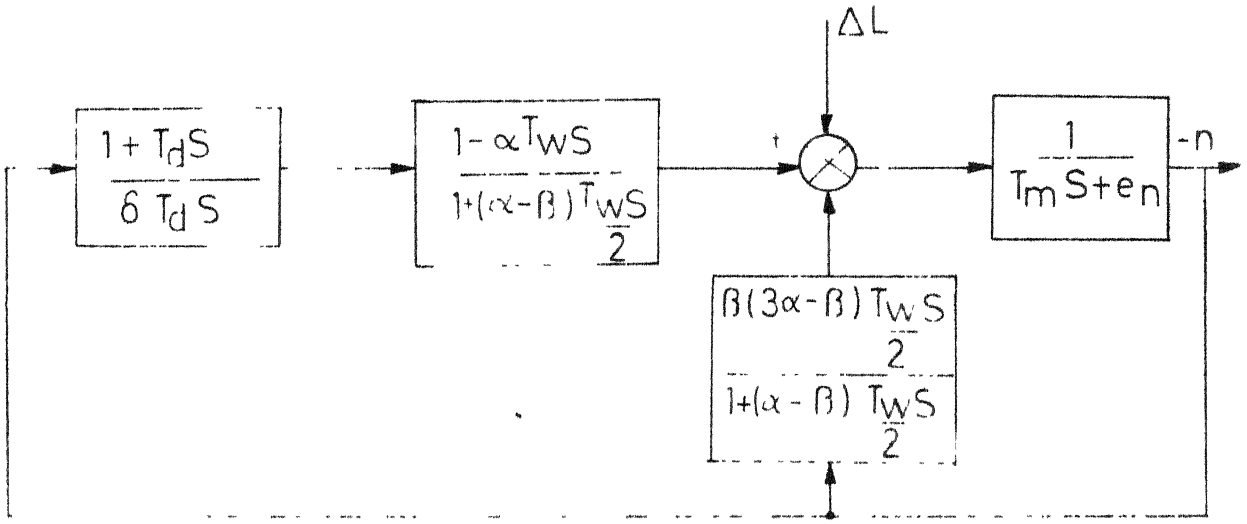

(a) Block diagram

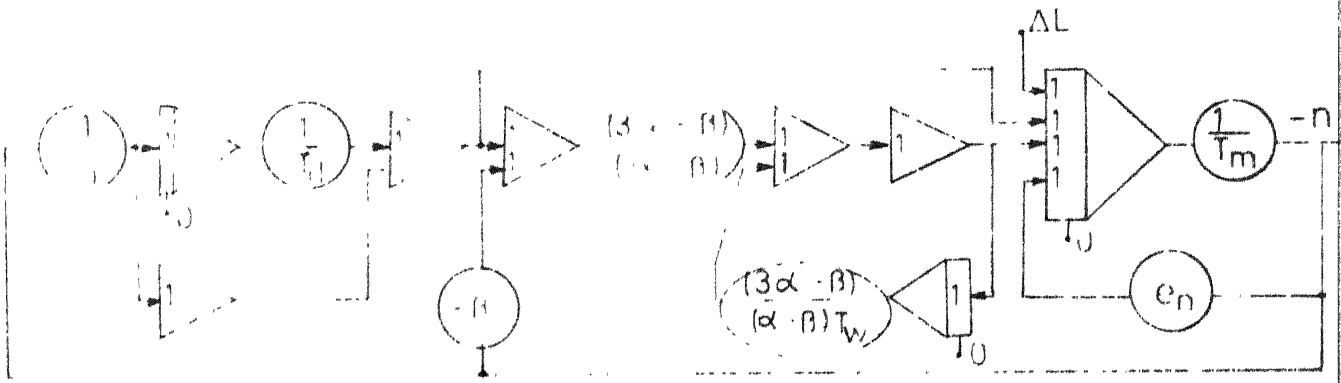

(b) State variable diagram

FIG·4 HYDRO-ELECTRIC GOVERNOR SYSTEM

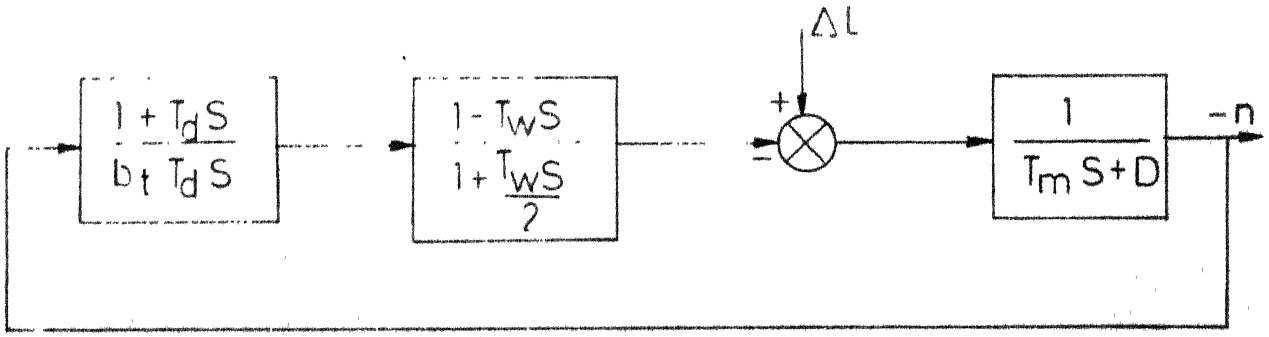

FIG. 5 CLASSICAL MODEL OF HYDRO-ELECTRIC GOVERNOR SYSTEM

2.3 Comparison with Classical Model

The conventional block diagram representation that considers approximate turbine transfer function (classical model of turbine), as used by Pai and Ganesan [2] is given in Figure 5 where D is considered as load damping factor.

When the conventional block diagram is compared with that given in Figure 4a, which takes into account true turbine characteristics, the following conclusions confirm the identities.

(i) At rated load the value of $\alpha = 1.0$ (as per the Figure A.5). While approximate turbine model is considered, it is assumed that flow does not depend on speed and so the value of $\beta = 0$. With these values of α and β, it can be seen that the true transfer function of turbine in Figure 4a will reduce to the classical turbine transfer function shown in Figure 5.

(ii) Referring to Figure A.5, if it were to be assumed as an approximation for turbine characteristics that the rate of change of RUQ and RUT with servo-positions is uniform throughout the range of servo-openings (instead of servo-positions around the region of peak efficiency), then the slope γ of effective gate will be equal to one. In that case there is no need for defining effective

temporary droop δ and the transfer function of governor in Figure 4a will be same as that given in Figure 5.

(iii) In Figure 5, D is considered as the load damping factor, where as in Figure 4a, corresponding to D in the transfer function of the system we have e_n - the overall coefficient of self-regulation of the system compromising self-regulation of the turbine as well as that of load and is given by

$$e_n = e_t - e_g \tag{6}$$

2.4 Comparison with Another Model [3]

Another linearized accurate model of a water turbine is given by Ramey and Skooglund [3]. The equations of quantity and torque that define the turbine-penstock transfer function are

$$q = a_{11} Z + a_{12} n + a_{13} \Delta s \tag{7}$$

$$\Delta m = a_{21} Z + a_{22} n + a_{23} \Delta s \tag{8}$$

where a_{11} is the partial derivative of turbine flow with respect to turbine head,

a_{12} is the partial derivative of turbine flow with respect to turbine speed,

a_{13} is the partial derivative of turbine flow with respect to gate position,

a_{21} is the partial derivative of turbine torque with respect to turbine head,

a_{22} is the partial derivative of turbine torque with respect to turbine speed,

a_{23} is the partial derivative of turbine torque with respect to gate position.

The corresponding equations of quantity and torque that are given by Goldwag [1] are

$$q = \gamma \Delta s + \frac{(\alpha - \beta)}{2} Z + \beta n \qquad (9)$$

$$\Delta m = \gamma \Delta s + \frac{(3\alpha - \beta)}{2} Z - (\alpha - \beta) n \qquad (10)$$

It can be seen that the two sets of eqns.(7), (8) and (9),(10) are identical for the following relationships of their coefficients.

$$\begin{aligned} a_{13} &= a_{23} = \gamma \\ a_{11} &= (\alpha-\beta)/2 \\ a_{21} &= (3\alpha-\beta)/2 \\ a_{12} &= \beta \\ a_{22} &= -e_t = -(\alpha-\beta) \end{aligned} \qquad (11)$$

However, the equations given by Goldwag are more realistic in the sense that the coefficients are defined in terms of the turbine characteristics that will normally be available, whereas the coefficients in the eqns. (7) and (8) are to be determined experimentally for the particular installation under study.

CHAPTER 3

SIMULATION OF THE HYDRO-ELECTRIC GOVERNOR SYSTEM

3.1 Range of Variations of Different Parameters

In order to simulate the hydro-electric governor system as represented in Figure 4, the range of variations of different parameters are to be known, which are as follows:

(i) β - the slope of RUG versus RUS characteristic:

For low head water turbine machines the value of β is greater than zero and for high head machines β is less than zero. Hence to cover all types of turbines the range of β that can be considered accordingly is

$$-1.0 \leq \beta < +1.0 \qquad (12)$$

at rated load when $\alpha = 1.0$.

(ii) α - the relative effective gate:

The value of effective gate at rated load is equal to one. Since our investigation is around the gate at which peak efficiency is obtained, effective gate values around one are considered. The range of values considered is from 0.9 to 1.05 as obtained from Figure A.5.

(iii) T_w, T_m - Time constants of water and turbine respectively:

Following typical values are assumed for T_w and T_m as considered by Pai and Ganesan [2]

T_w - water starting time = 1.24 secs.

T_m - Machine starting time = 9.05 secs.

The values of T_w and T_m depend on the particular installation for which stability analysis has to be made.

(iv) e_n - the coefficient of self-regulation:

The effect of e_n can usually be neglected since the self-regulation is more system than characteristic dependent and depending on the type of load carried the overall effect of turbine and load self-regulations may become zero. The value of e_n can vary from zero to one.. Goldwag has neglected e_n in his theoretical investigation of stability of the system.

(v) δ, T_d - effective temporary droop and dashpot time constants:

Particular values of δ and T_d constitute the optimum setting of governor based on the criterion used for the same. To obtain the limit of stability curves, δ and T_d are to be varied simultaneously over a range of values. For this a range from 0.1 to 2.0 for δ and a range from 0 to 1.0 for T_d can be considered. T_d value can go up to 2 or 3 in case the damping factor or self-regulation coefficient is not neglected. These ranges of δ and T_d are assumed based on the theoretical results as obtained by Goldwag[1] and Pai and Ganesan[2].

3.2 Analog Simulation Results

Analog simulation of the hydro-electric governor system as represented in Figure 4 is carried out using AC-20 analog computer. The experimental set up is shown in Figure 6. A step load change Δ L of 10 percent is considered.

Theoretically the limit of stability curves, as derived by Goldwag, are defined by a relation (Appendix B) given by

$$X_2 = \frac{1 - X_1}{K - X_1} \tag{13}$$

where

$$X_1 = \frac{\alpha T_w}{\delta T_m} - \frac{\alpha T_w}{T_m} \beta K \tag{14}$$

$$X_2 = \alpha \frac{T_w}{T_d} \tag{15}$$

and

$$K = \frac{(3\alpha - \beta)}{2\alpha} \tag{16}$$

Numerical data derived from eqn.(13) is given in Table 1 from which theoretical limit of stability curves for various values of β can be drawn as shown in Figure 7.

Critical damping conditions are derived by Goldwag (Appendix B), which are as follows

$$9(K-1)X_2 = (1-X_1)(1-X_2) \tag{17}$$

$$3(K-1)(1-X_2) = \frac{(1 - X_1)^2}{\alpha \frac{T_w}{T_m} \beta K + X_1} \tag{18}$$

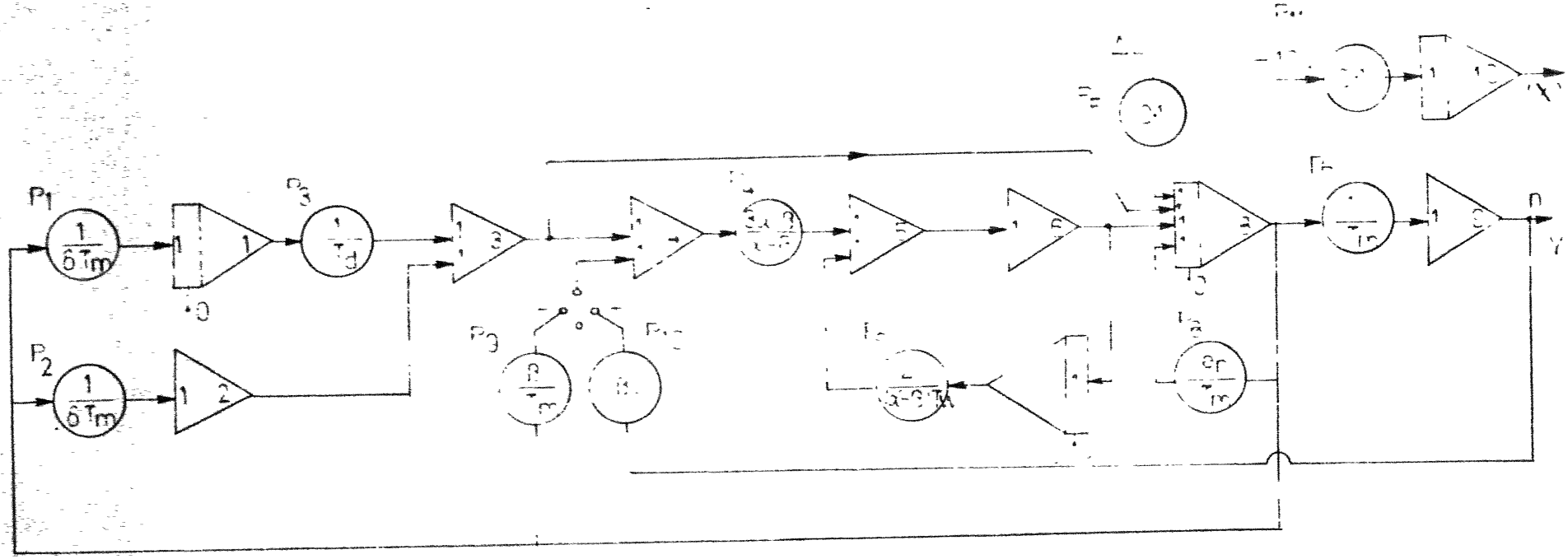

FIG.6 ANALOG SIMULATION SET UP OF HYDRO-ELECTRIC GOVERNOR SYSTEM ON AC-20 COMPUTER

Table 1: Data for Theoretical Limit of Stability Curves at Rated Load.

$\alpha = 1, \quad e_n = 0$

	$\beta = 0.0$			$\beta = -0.5$			$\beta = +0.5$		
X_1	δ	X_2	$1/T_d$	δ	X_2	$1/T_d$	δ	X_2	$1/T_d$
0.0	∞	0.667	0.538	-	0.571	0.460	1.592	0.800	0.645
0.1	1.370	0.643	0.518	-	0.545	0.440	0.738	0.783	0.630
0.2	0.685	0.615	0.495	1.712	0.516	0.416	0.470	0.762	0.615
0.3	0.457	0.584	0.470	0.760	0.483	0.389	0.356	0.737	0.595
0.4	0.342	0.545	0.440	0.490	0.445	0.358	0.282	0.705	0.568
0.5	0.274	0.500	0.403	0.361	0.400	0.322	0.234	0.667	0.538
0.6	0.228	0.445	0.358	0.286	0.348	0.281	0.200	0.615	0.495
0.7	0.196	0.375	0.302	0.236	0.286	0.231	0.175	0.545	0.440
0.8	0.171	0.286	0.231	0.202	0.210	0.169	0.155	0.445	0.358
0.9	0.152	0.167	0.135	0.176	0.118	0.095	0.139	0.286	0.231
1.0	0.137	0.000	0.000	0.156	0.000	0.000	0.126	0.000	0.000

Equation (17) will define the curves corresponding to the critical damping points and eqns.(17) and (18) together when solved, will give the governor setting values for critical damping. The governor settings corresponding to critical damping condition for three types of turbines, i.e., for three values of β at rated load when $\alpha = 1.0$ are calculated which arepresented in Table 2. Numerical data as calculated from eqn.(17) is also presented in Table 3 from which the critical damping curves can be drawn as shown in Figure 7. According to Goldwag the optimum setting of governor for a particular turbine will lie some where in between the limit of stability curve and the curve corresponding to the critical damping point.

Table 2: Governor Settings for Critical Damping Condition

Type of turbine β	Effective temporary droop δ	Inverse of dashpot time constant $1/T_d$
0.0	0.4050	0.1035
-0.5	0.6370	0.0723
+0.5	0.2600	0.1610

During the course of simulation of the system on analog computer, the limit of stability curves for various machines are obtained and also the effect of not

Table 3: Data for Theoretical Curves Corresponding to Critical Damping at rated load.

$\alpha = 1.0$, $e_n = 0.0$

	$\beta = 0.0$			$\beta = -0.5$			$\beta = +0.5$		
X_1	δ	X_2	$1/T_d$	δ	X_2	$1/T_d$	δ	X_2	$1/T_d$
0.0	∞	0.182	0.147	-	0.129	0.104	1.592	0.308	0.248
0.1	1.370	0.167	0.134	-	0.118	0.095	0.738	0.277	0.224
0.2	0.685	0.151	0.122	1.712	0.106	0.086	0.470	0.262	0.211
0.3	0.457	0.135	0.108	0.760	0.094	0.076	0.356	0.237	0.191
0.4	0.342	0.118	0.095	0.490	0.082	0.066	0.282	0.205	0.165
0.5	0.274	0.100	0.081	0.361	0.069	0.056	0.234	0.182	0.147
0.6	0.228	0.082	0.066	0.286	0.056	0.045	0.200	0.151	0.122
0.7	0.196	0.063	0.050	0.236	0.043	0.034	0.175	0.118	0.095
0.8	0.171	0.043	0.034	0.202	0.029	0.023	0.155	0.082	0.066
0.9	0.152	0.022	0.018	0.176	0.015	0.012	0.139	0.043	0.034
1.0	0.137	0.000	0.000	0.156	0.000	0.000	0.126	0.000	0.000

neglecting e_n as well as the effect of changing α which means operating the machine at a load other than rated full load, are studied. The numerical data for limit of stability curves for three values of β at rated full load neglecting e_n as well as for $e_n = 1.0$, is given in Table 4. Variation of α is also considered the numerical data of which is given in Table 5. Various graphs are plotted as shown in Figures 7, 8 and 9. Transient response curves for the frequency state variable of the system for typical settings of governor are given in Figures 10 to 13.

3.3 Comments on the Analog Simulation Results

(i) It is observed that there is significant effect of the true turbine characteristics (β) on the region of stable operation of the turbine as illustrated in Figure 7. The limit of stability curves at rated load obtained by analog simulation of the system for three values of β agree with those obtained theoretically by Goldwag.

(ii) The optimum setting of the governor parameters δ and T_d based on any criterion will normally be in the region between the limit of stability curve and that corresponding to the point of critical damping.

(iii) It is obvious from the transient response curves given in Figures 10 to 13, that a particular governor setting on different types of turbines will give rise to different types of transient responses.

Table 4: Experimental data for Limit of Stability Curves at Rated Load.
$\alpha = 1.0$

		$\beta = 0.0$		$\beta = -0.5$		$\beta = +0.5$	
		$e_n=0$	$e_n=1$	$e_n=0$	$e_n=1$	$e_n=0$	$e_n=1$
$1/\delta T_m$	δ	$1/T_d$	$1/T_d$	$1/T_d$	$1/T_d$	$1/T_d$	$1/T_d$
0.070	1.580	0.522	1.380	0.414	1.080	0.642	1.700
0.100	1.100	0.507	1.100	0.405	0.878	0.638	1.360
0.120	0.920	0.505	-	0.398	-	0.634	-
0.150	0.736	0.494	0.880	0.387	0.713	0.629	1.100
0.180	0.614	0.488	0 -	0.376	-	0.624	-
0.200	0.552	0.482	0.776	0.370	0.612	0.621	0.978
0.250	0.442	0.465	-	0.345	-	0.608	-
0.300	0.368	0.447	0.640	0.325	0.489	0.595	0.829
0.400	0.276	0.395	--	0.271	-	0.569	0.735
0.500	0.221	0.341	0.463	0.204	0.315	0.524	0.656
0.600	0.184	0.266	0 -	0.119	-	0.462	0.571
0.700	0.157	0.155	-	-	-	-	-
0.705	0.156	-	-	0.000	-	-	-
0.786	0.141	-	-	-	0.000	-	-
0.796	0.139	0.000	-	-	-	-	-
0.800	0.138	-	-	-	-	0.206	0.305
0.860	0.129	-	0.000	-	-	-	-
0.870	0.127	-	-	-	-	0.000	-
0.900	0.123	-	-	-	-	-	0.000

Table 5: Experimental Data for Limit of Stability Curves at Loads Different from rated load.

		α=0.9, e_n=0.0			α = 1.05, e_n = 0.0		
		β=0	-0.5	+0.5	0.0	-0.5	+0.5
$1/\delta T_m$	δ	$1/T_d$	$1/T_d$	$1/T_d$	$1/T_d$	$1/T_d$	$1/T_d$
0.070	1.580	0.589	0.462	0.740	0.491	0.393	0.618
0.100	1.100	0.580	0.453	0.727	0.488	0.383	0.609
0.150	0.736	0.568	0.435	0.718	0.472	0.366	0.601
0.200	0.552	0.553	0.417	0.715	0.457	0.344	0.590
0.300	0.368	0.518	0.377	0.691	0.421	0.299	0.560
0.400	0.276	0.478	0.327	0.663	0.373	0.243	0.527
0.500	0.221	0.427	0.270	0.629	0.314	0.172	0.483
0.600	0.184	0.363	0.200	0.578	0.229	0.081	0.420
0.665	0.166	-	-	-	-	0.000	-
0.700	0.158	-	-	-	-	-	0.322
0.762	0.145	-	-	-	0.000	-	-
0.800	0.138	0.166	0.000	0.402	-	-	0.133
0.840	0.132	-	-	-	-	-	0.000
0.900	0.123	0.000	-	0.214	-	-	-
0.962	0.115	-	-	0.000	-	-	-

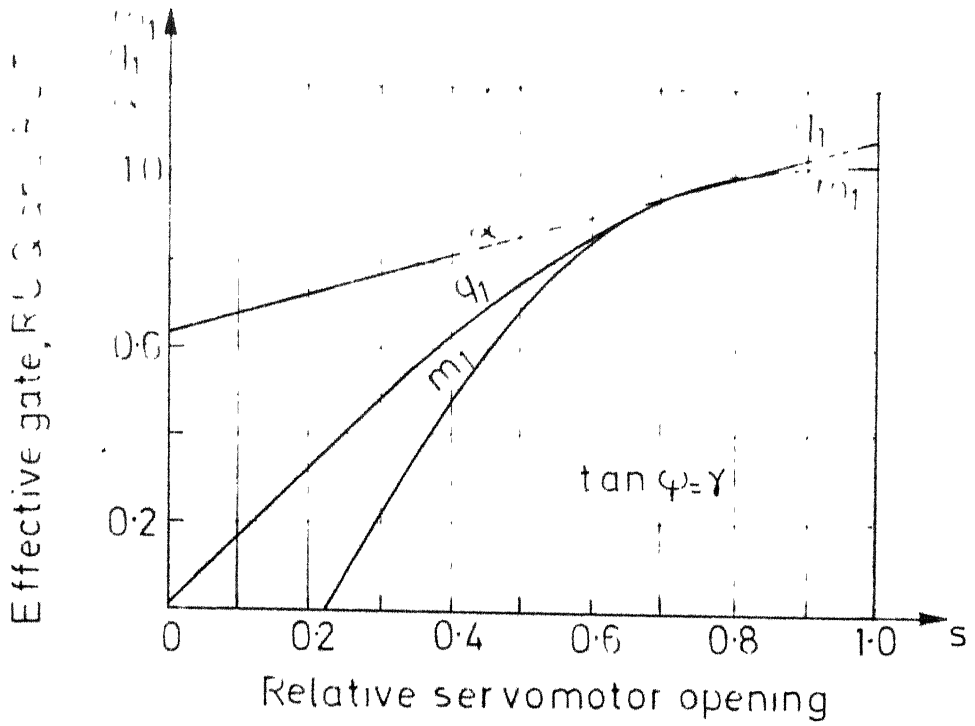

FIG. A-5 RELATIONSHIP BETWEEN GATE, TORQUE, AND FLOW AT CONSTANT UNIT SPEED

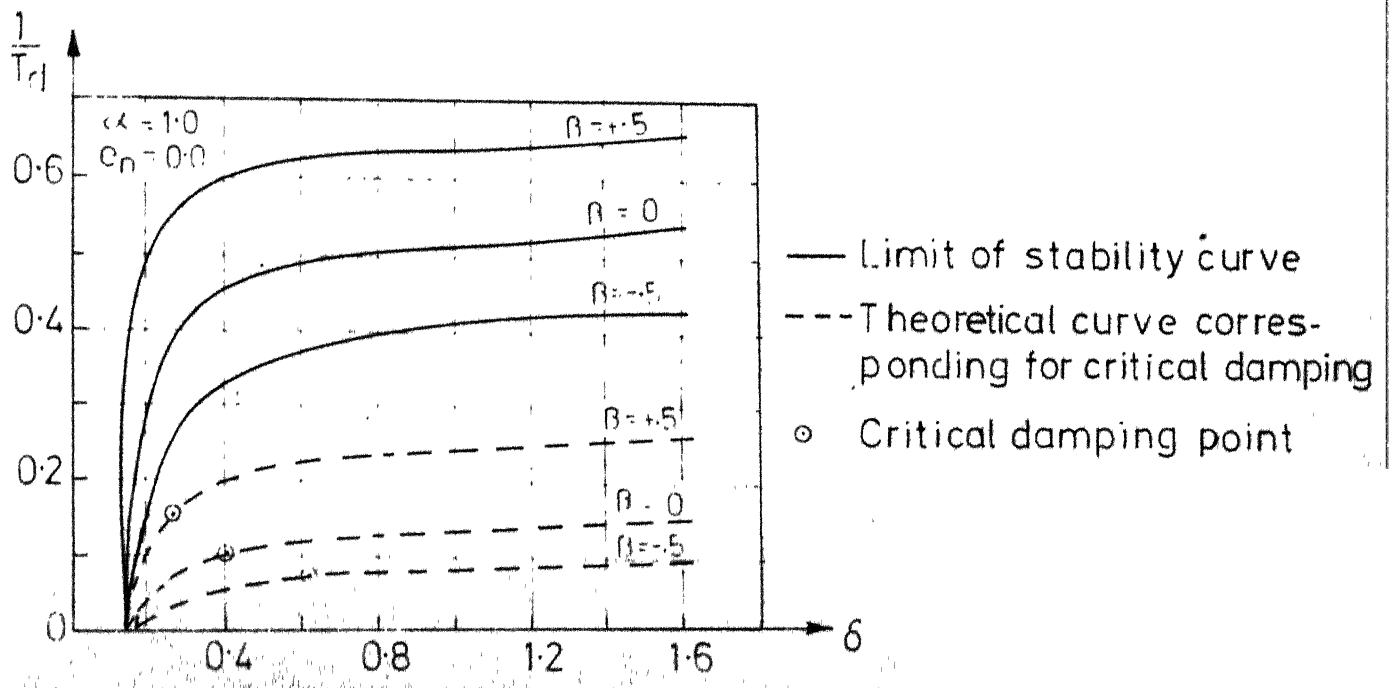

FIG. 7

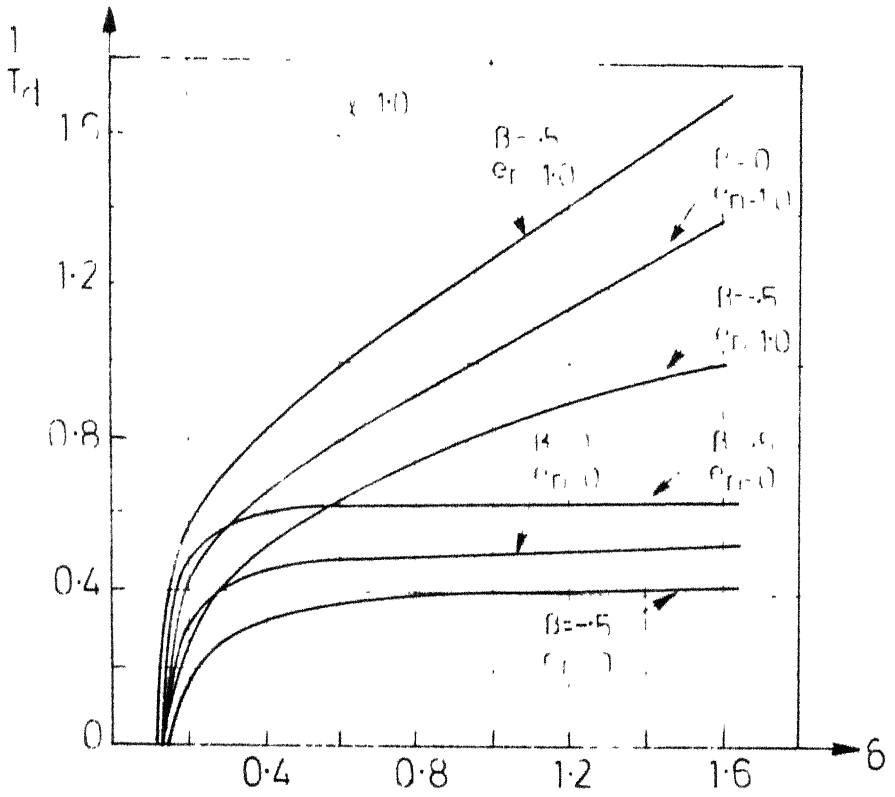

FIG·8 LIMIT OF STABILITY CURVES

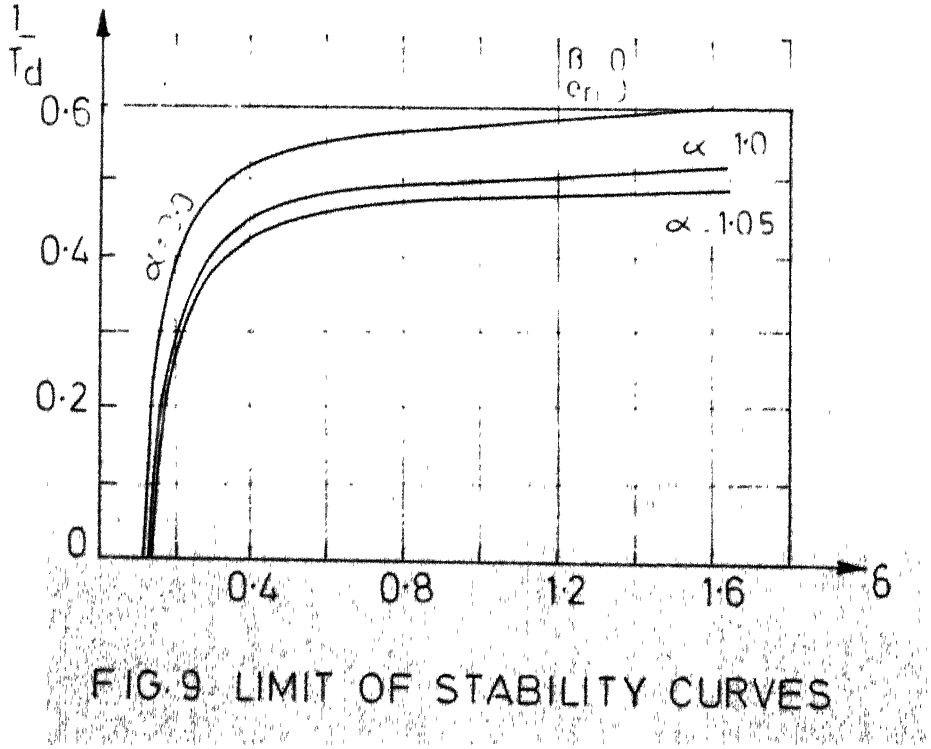

FIG·9 LIMIT OF STABILITY CURVES

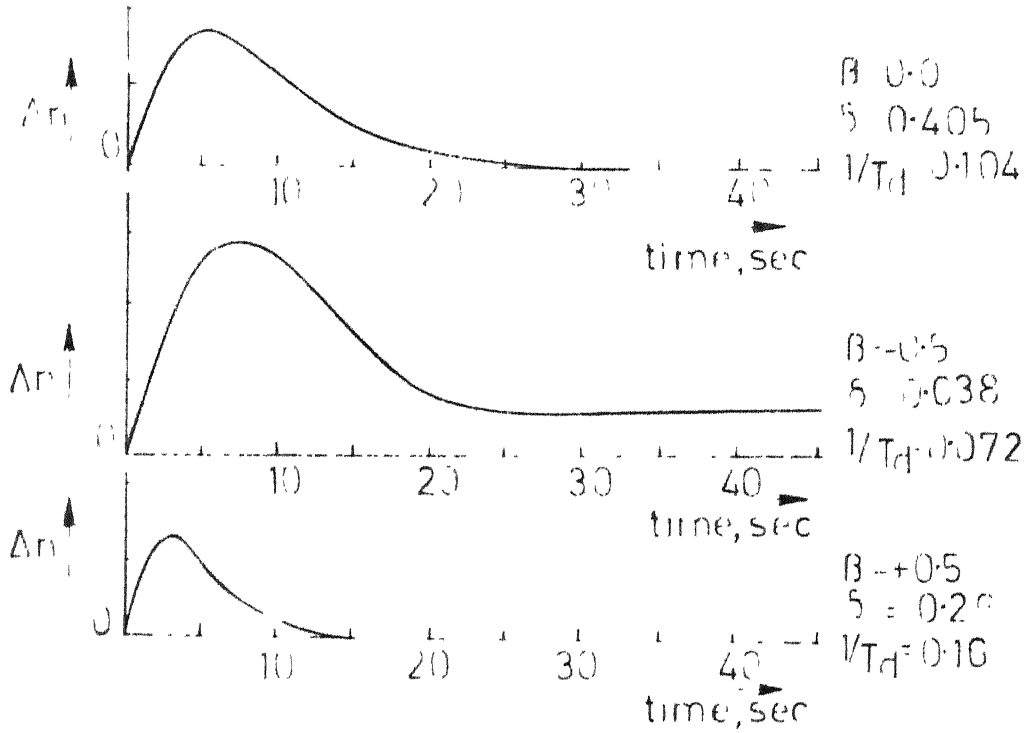

FIG 10 TRANSIENT RESPONSE AT CRITICAL DAMPING POINTS (THEORETICAL) AS PER GOLDWAG

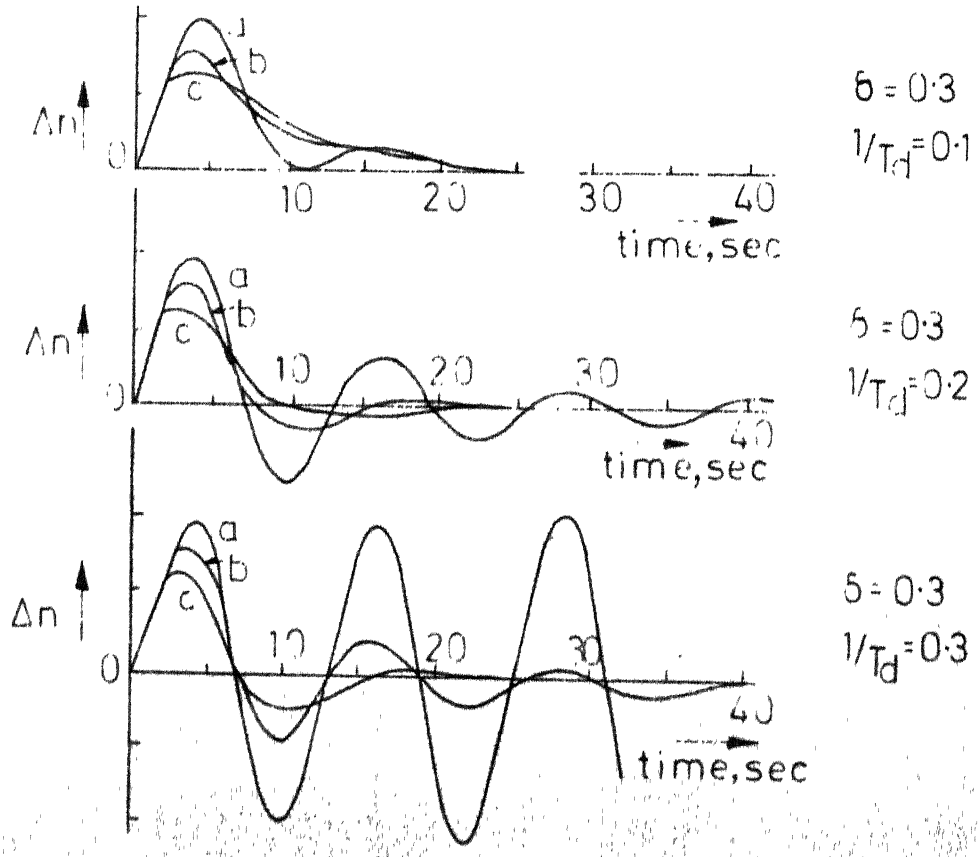

FIG 11 TRANSIENT RESPONSE FOR (a) β=-0·5, (b) β=0, (c) β=+0·5

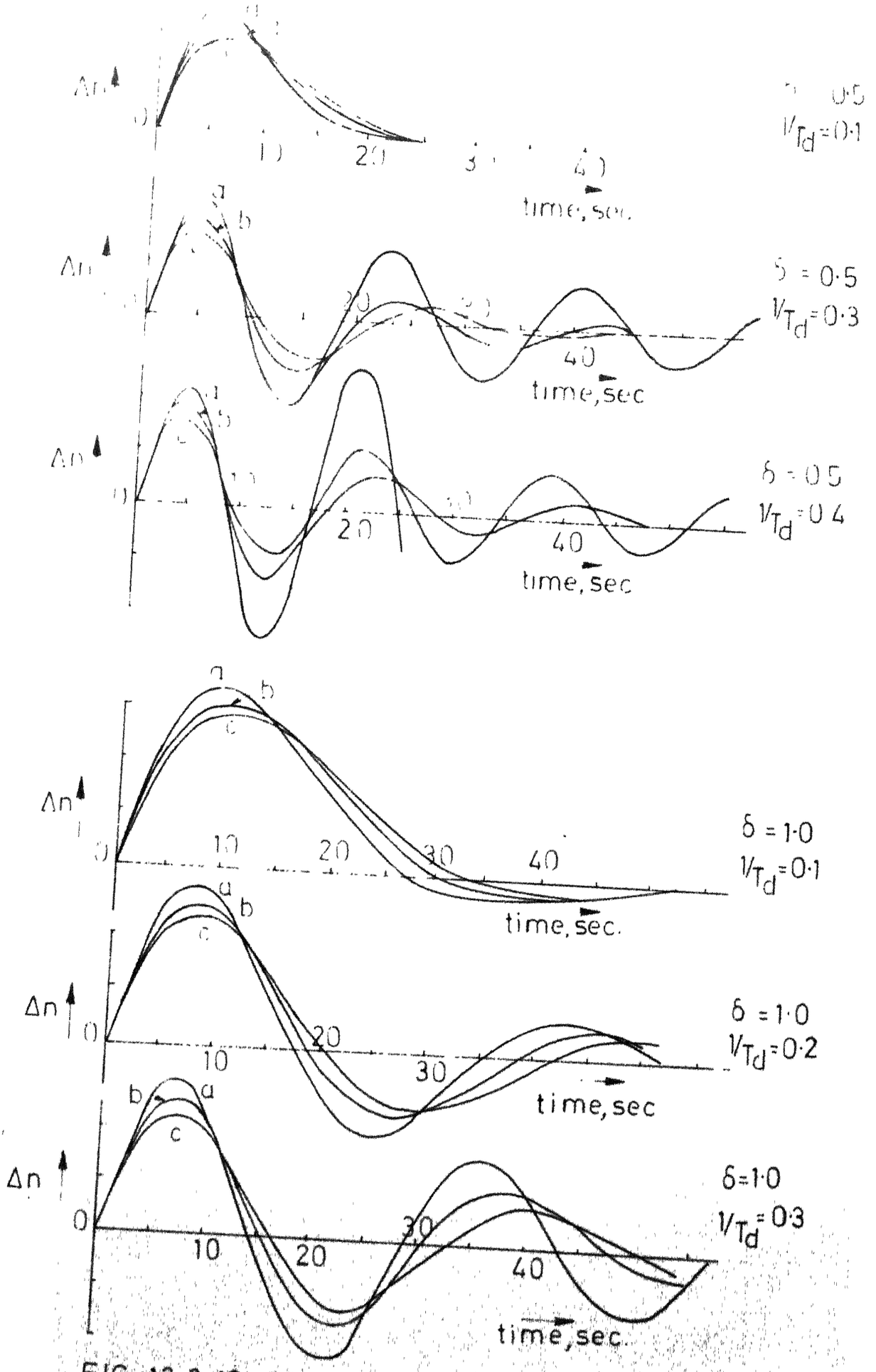

FIG. 12 & 13 TRANSIENT RESPONSE FOR (a) β=-0·5, (b) β= 0, (c) β=+0·5

(iv) For gate openings different from that at rated load, we observe from Figure 9 that the region of stable operation becomes smaller for higher values of gate openings and becomes larger for lower values.

(v) If the damping coefficient e_n was not to be neglected, we observe from Figure 8 that the region of stable operation increases. This result agrees with that obtained by Pai and Ganesan [2].

CHAPTER 4

CONCLUSION

Diagrammatic representation of hydro-electric governor system, taking true turbine characteristics into account, is developed making use of the mathematical model given by Goldwag [1]. Analog simulation studies are carried out for a particular case using AC-20 analog computer. The theoretical results obtained earlier by Goldwag [1] and Pai and Ganesan [2] are verified, showing the significant effect of turbine characteristics on the stability of the system.

APPENDIX A

DERIVATION OF TURBINE SYSTEM TRANSFER FUNCTION MAKING USE OF TURBINE CHARACTERISTICS

The basic differential equations of the water turbine system are derived by Goldwag [1] from the information of the following turbine characteristics.

(i) Relative unit quantity (RUQ) versus relative unit speed (RUS).

(ii) Relative unit torque (RUT) versus RUS

(iii) Relative servo opening (RSO) versus RUQ and RUT

which are given in Figures A.1, A.2 and A.5. It can be observed that these turbine characteristics can very closely be represented by straight line tangents at the point corresponding to the unit speed as shown in Figures A.3, A.4 and A.5. The derivation of the turbine system equations are as follows.

Equation of Flow

Referring to Figure A.3 the RUQ (q_1) at given gate Y_r and RUS(n_1) is given by

$$q_1 = q_{1r} + \beta\ (n_1 - 1) \qquad (A.1)$$

and the relative quantity (q) at head deviation Z is

$$q = q_1 \sqrt{1+Z}$$

$$= q_{1r} \sqrt{1+Z} + \beta(1+n - \sqrt{1+Z}) \qquad (A.2)$$

after substituting for n_1 given by

$$n_1 = (1+n)/\sqrt{1+Z} \qquad (A.3)$$

This can be rearranged as

$$q = (q_{1r}-\beta)\sqrt{1+Z} + \beta(1-n) \qquad (A.4)$$

The conventional form of the eqn.(A.4) is

$$q = q_{1r}\sqrt{1+Z} \qquad (A.5)$$

Comparing eqns. (A.4) and (A.5), we see that eqn.(A.5) completely neglects the speed dependence of flow. Secondly, when eqn.(A.5) is used to represent propellers and low head machines, it over-estimates the effect of pressure changes of flow.. When used to represent high head machines, it under-estimates the dependence of flow on the pressure. Eqn.(A.5) was first derived for Pelton machines and hence it represents correctly the flow for such medium head machines..

The value of β - the slope of RUQ versus RUS characteristic, represents to some scale a measure of the error in the dependence of the quantity on pressure changes and also represents to scale the speed dependence of flow.

Equation of Torque:

Referring to Figure A.4 the RUT (m_1) at a given gate Y_r and RUS is given by

$$m_1 = m_{1r} - e_t(n_1 - 1) \qquad (A.6)$$

where e_t - the slope, represents the coefficient of self-regulation of the turbine and is given by

$$e_t = m_{1r}/R \qquad (A.7)$$

where R is the relative speed deviation at the extrapolated runaway speed and rated load.

The relative torque at head deviation Z is given by

$$m = m_1(1+Z) \qquad (A.8)$$

$$= m_{1r}\left[\frac{(R+1)(1+Z)-\sqrt{1+Z}}{R}\right] - \frac{m_{1r}}{R}\, n\sqrt{1+Z} \qquad (A.9)$$

The first term in eqn.(A.9) represents the dependence of torque on pressure and the second term the inherent self-regulation of the turbine.

When relative pressure change is small and if its effect on turbine self-regulation is neglected, eqn.(A.9) can be reduced to a more manageable form

$$m_1 = m_{1r}(1+KZ) - e_t n \qquad (A.10)$$

where

$$K = 1 + \frac{1}{2R}$$

For Pelton and medium head machines the value of K = 3/2 and therefore, the conventional form of torque equation is

$$m_l = m_{lr}\left(1 + \frac{3Z}{2}\right) - e_t n \qquad (A.11)$$

and for other machines the value of K is to be properly chosen.

Relative effective gate

Now we introduce the concept of relative effective gate which facilitates in connecting the parameters of the derived eqns.(A.4) and (A.10) to the gate, thereby reducing the number of parameters.

For any turbine, as shown in Figure A.5, it is seen that over a range of servomotor positions around the region of peak efficiency, the RUQ and RUT are approximately equal and have equal rate of change with servo position. Now, if we define relative effective gate in this region by the expression

$$\alpha = g + \gamma s \qquad (A.12)$$

where γ is the slope of effective gate versus RSO, then we have

$$\alpha = q_{lr} = m_{lr} = g + \gamma s \qquad (A.13)$$

and

$$\gamma = \frac{\Delta \alpha}{\Delta s} = \frac{\Delta q_{lr}}{\Delta s} = \frac{\Delta m_{lr}}{\Delta s} \qquad (A.14)$$

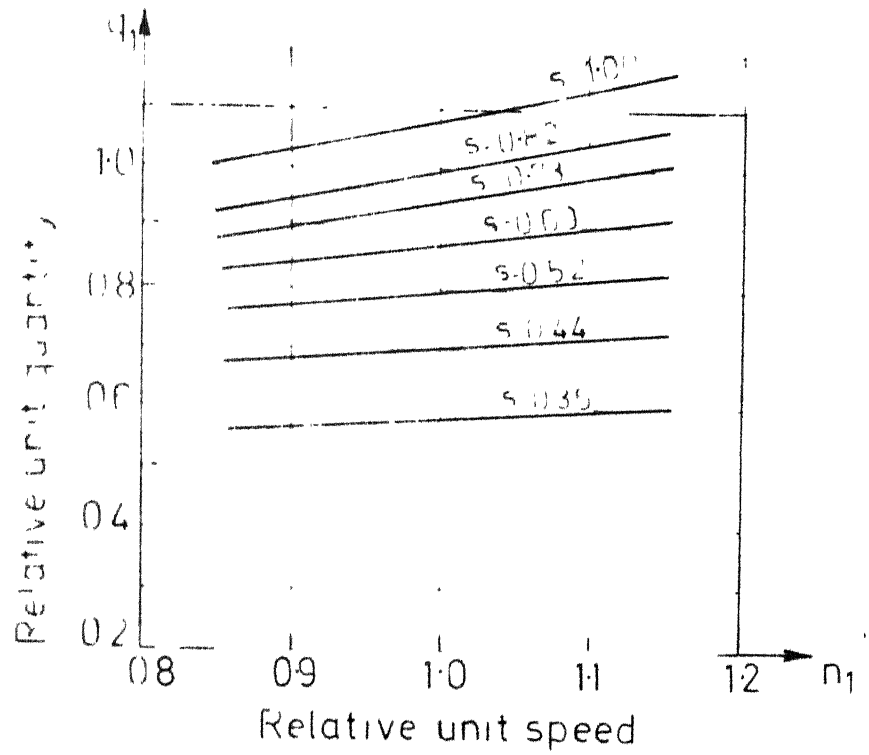

FIG.A1 TYPICAL FLOW CHARACTERISTICS

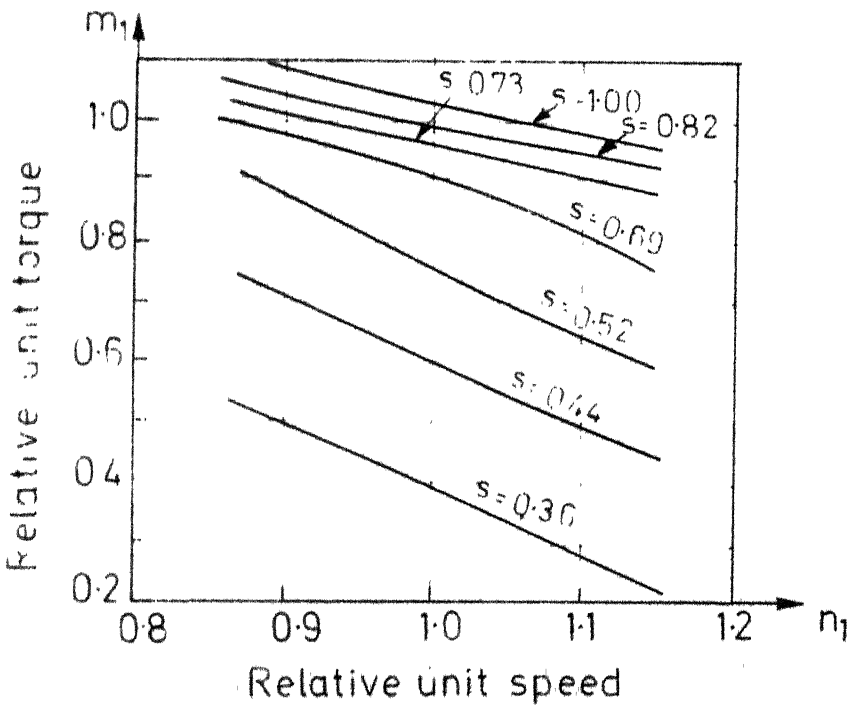

FIG. A-2 TYPICAL TORQUE CHARACTERISTICS

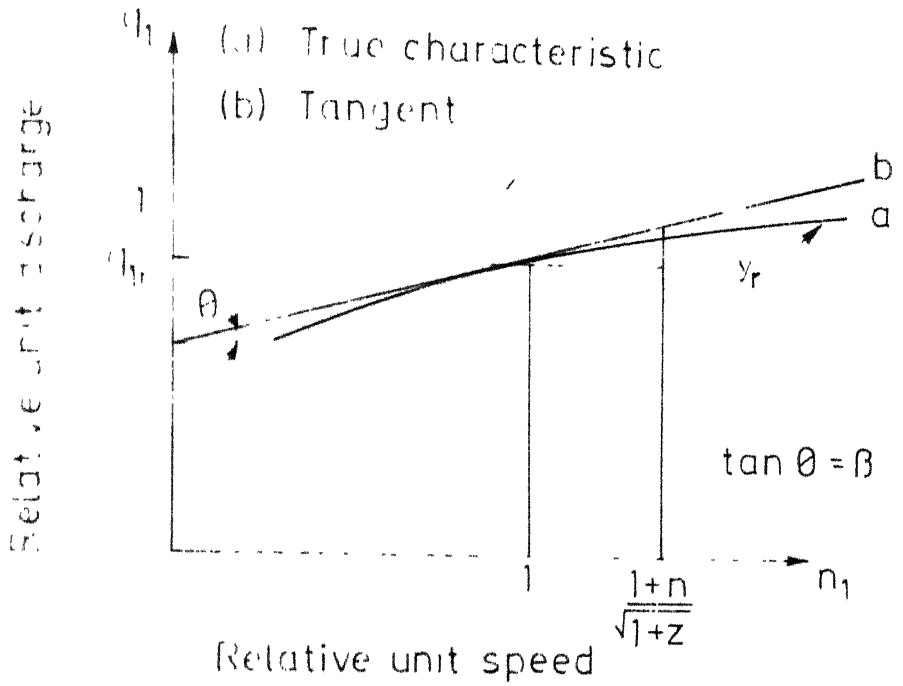

FIG. A-3 DERIVATION OF EQUATION OF FLOW

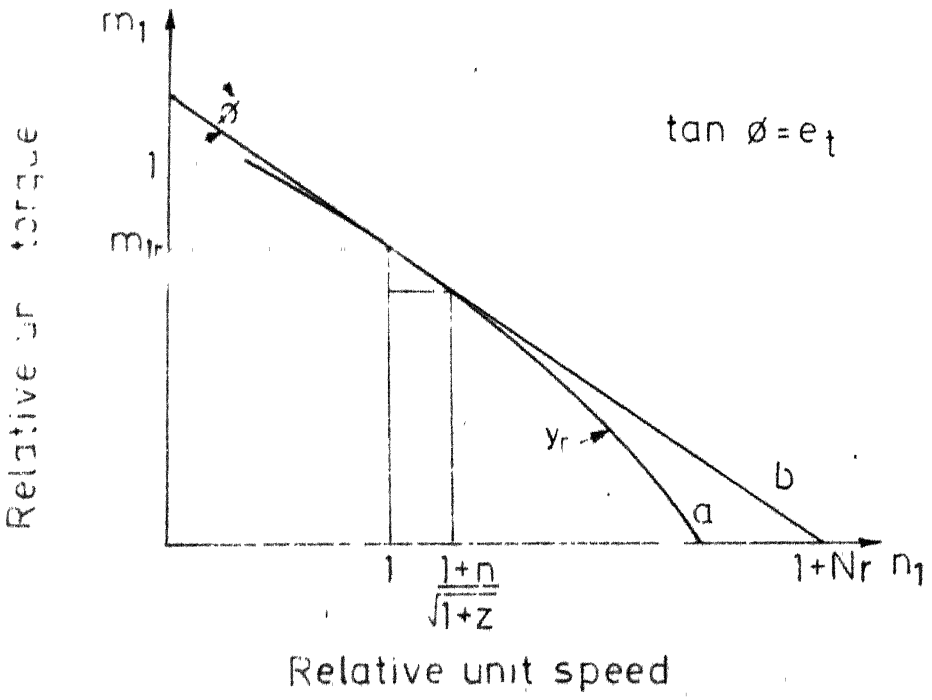

FIG. A-4 DERIVATION OF TORQUE EQUATION

Differential equations of the turbine system

If the changes in quantity and torque are small, then the efficiency of the unit can be assumed to be constant throughout the changes and the torque and quantity characteristics can be related by

$$M = \frac{Q\,H}{N}\,\eta \qquad (A.15)$$

from which the difference equation

$$\Delta m = \gamma \Delta s + \frac{(3\alpha - \beta)}{2} Z - (\alpha-\beta)n \qquad (A.16)$$

can be derived. Comparing eqns.(A.10) and (A.16) and making use of eqns.(A.13) and (A.14), we get

$$R = \alpha/(\alpha-\beta) \qquad (A.17)$$

$$e_t = \alpha-\beta \qquad (A.18)$$

$$K = 1 + \frac{(\alpha-\beta)}{2\alpha} = \frac{(3\alpha-\beta)}{2\alpha} \qquad (A.19)$$

With the help of eqns.(A. 4), (A.10), (A.14) and (A.16), we can write the two basic differential equations of the turbine system as follows:

$$-\frac{Z}{T_w} = \frac{dq}{dt} = \gamma \frac{d(\Delta s)}{dt} + \frac{(\alpha-\beta)}{2}\frac{dZ}{dt} + \beta \frac{dn}{dt} \qquad (A.20)$$

$$T_m \frac{dn}{dt} = \gamma \Delta s + \frac{(3\alpha-\beta)}{2} Z - [(\alpha-\beta)-e_g]n \qquad (A.21)$$

subject to the assumptions that the slope of RUQ versus

RUS characteristics does not vary significantly with gate and the bulk water hammer represents adequately the pressure changes following variations of flow.

Differential equation of governor

The transfer function of a sensitive governor (infinite gain is assumed) equipped with temporary and permanent droops is

$$\Delta s = - \frac{1+T_d S}{b_p\left[1+\left(\frac{b_t + b_p}{b_p}\right) T_d S\right]} n \qquad (A.22)$$

where $\left(\frac{b_t+b_p}{b_p}\right) T_d$ is termed as 'on load' time constant and S is the Laplace operator.

Since our main interest is to show the effect of the true turbine characteristics, we assume the most basic form of transfer function of the governor (permanent droop neglected) as

$$\Delta s = - \frac{(1 + T_d S)}{b_t T_d S} n \qquad (A.23)$$

The eqns.(A.20), (A.21) and (A.23) represent mathematically the isolated hydro-electric governor system under consideration.

APPENDIX B

THEORETICAL RESULTS AS OBTAINED BY GOLDWAG[1]

Limit of stability

Combining eqns.(A.20), (A.21) and (A.23), the characteristic equation of the system can be derived as

$$\frac{(\alpha-\beta)}{2}\,\delta T_m T_w\, S^3 + \delta T_m\left[1 - \frac{\alpha\, T_w}{\delta\, T_m}\,(1-\delta K\beta-\delta(K-1)e_n)\right] S^2 + \left(1 + \delta e_n - \frac{\alpha\, T_w}{T_d}\right) S + \frac{1}{T_d} = 0 \qquad \text{(B.1)}$$

Coefficient of self-regulation, e_n can normally be neglected. Then the system characteristic equation is

$$\frac{(\alpha-\beta)}{2}\,\delta T_m T_w\, S^3 + \delta T_m\left[1 - \frac{\alpha\, T_w}{\delta\, T_m}(1 - \delta K\beta)\right]S^2 + \left(1 - \frac{\alpha\, T_w}{T_d}\right)S + \frac{1}{T_d} = 0 \qquad \text{(B.2)}$$

For a third order system, the characteristic equation of which can be represented as

$$A_3\, S^3 + A_2\, S^2 + A_1\, S + A_o = 0 \qquad \text{(B.3)}$$

the system can be stable if the following conditions (Routh-Hurwitz) are satisfied.

$$A_3 \geq 0,\quad A_2 \geq 0,\quad A_1 \geq 0,\quad A_o \geq 0 \text{ and}$$

$$A_2 A_1 \geq A_3 A_o \qquad \text{(B.4)}$$

applying these conditions to the system characteristic equation (B.2) and observing that at the limit of stability boundary $A_2 A_1 = A_3 A_0$, an expression, which defines the limit of stability curve for the system, can be derived as

$$X_2 = \frac{1 - X_1}{K - X_1} \tag{B.5}$$

where

$$X_1 = \frac{\alpha T_w}{\delta T_m} - \frac{\alpha T_w}{T_m} \beta K \tag{B.6}$$

$$X_2 = \frac{\alpha T_w}{T_d} \tag{B.7}$$

and K is as given by eqn.(A.19). The expression (B.5) defines the limit of stability curves for various values of β/α or for various β (i.e., different types of machines) at rated load when $\alpha = 1.0$.

Critical damping

The critical damping conditions for the third order system are

$$A_2^2 = 3A_1A_3 \tag{B.8}$$

$$A_2^3 = 27A_0A_3^2 \tag{B.9}$$

Applying these conditions to the system (B.2), two relationships

$$9(K-1)\frac{X_2}{(1-X_2)} = (1-X_1) \qquad \text{(B.10)}$$

$$3(K-1)(1-X_2) = \frac{(1-X_1)^2}{\left(\frac{\alpha}{T_m}\frac{T_w}{}\beta K + X_1\right)} \qquad \text{(B.11)}$$

are obtained, which on solving, will give the values of governor parameters δ and T_d at the point of critical damping. Eqn.(B.10) alone defines the curves corresponding to the critical damping point.

REFERENCES

1. Goldwag, E., 'On the influence of water turbine characteristics on stability and response', Trans. of ASME, Journal of Basic Engineering, 1971, pp. 481-494.

2. Pai, M.A., and Ganesan, K., 'Relative stability of load-frequency control systems', IEEE Trans. Power Apparatus and Systems, 1971, pp. 2734-2741.

3. Ramey, D.G., and Skooglund, J.W., 'Detailed hydro-governor representation for system stability studies', IEEE Trans. Power Apparatus and Systems, 1970, pp. 106-112.

4. Jagdish Lal, Hydraulic Machines, 1959, Metropolitan Book Co. Pvt.Ltd., Delhi.

5. Kuo, B.C., Automatic Control Systems, 1969, Prentice-Hall, New Delhi.

6. Tou, J.T., Modern Control Theory, 1964, McGraw-Hill, New York.

PART B

MODAL CONTROL OF A POWER SYSTEM

CHAPTER 1

INTRODUCTION

In the recent years the optimal linear regulator theory for linear, time-invariant systems with quadratic performance indices has been applied to design controllers for power systems for obtaining improved dynamic behaviour of these systems [1,10,11]. Yu et al [1] considered a power system consisting of a synchronous machine connected to an infinite bus through a transmission line, along with the exciter-voltage regulator and governor-hydraulic systems. The eighth order nonlinear mathematical model describing this system was linearized around an operating point to obtain a linear, time-invariant state model of the power system, valid for small disturbances. This is represented by the standard notation given in equation (1)

$$\dot{\underline{x}}(t) = A\,\underline{x}(t) + B\,\underline{u}(t) \qquad (1)$$

Defining the optimal state regulator problem for this system with the quadratic performance index

$$J = \int_0^\infty (\underline{x}'\,Q\,\underline{x} + \underline{u}'R\,\underline{u})dt \qquad (2)$$

where Q and R are symmetric, positive definite matrices. Yu et al derived a feedback control law in the form

$$\underline{u}(t) = -R^{-1}\,B'\,K\,\underline{x}(t) \qquad (3)$$

The nxn 'gain' matrix K is the positive definite solution to the matrix equation

$$A' K + K A - K B R^{-1} B' K + Q = [0] \qquad (4)$$

The resulting closed-loop defined by the equation

$$\dot{\underline{x}}(t) = (A - B R^{-1} B' K) \underline{x}(t) \qquad (5)$$

is a stable system with better dynamic response than the uncontrolled system given by eqn.(1).

It is to be noted that there is no apriori knowledge of what the matrices Q and R should be in order to obtain the desired closed-loop system behaviour. The closed-loop system behaviour is judged in terms of its transient response characteristics as in classical servo-system design methods, and this behaviour depends mainly on the location of the eigenvalues of the closed-loop system. It has thus been necessary for Yu et al to systematically change the Q and R matrices till a satisfactory closed-loop behaviour is obtained. It is better to employ design techniques which directly yield the required closed-loop eigenvalue locations of the system. This would avoid the problem of having iteratively to solve a sequence of optimal, linear regulator problems as done by Yu et al.

In contrast to the above design technique, in the modal control approach, the desired locations of the closed-loop system eigenvalues can be specified and state

variable feedback loops can be directly designed to shift the eigenvalues of the open-loop system to the desired locations [2,3,4,5]. It is well known that it is possible to achieve any arbitrarily assigned closed-loop eigenvalue locations (with the constraint that complex eigenvalues should occur in conjugate pairs) if the open-loop system is controllable [9]. However, in many practical situations, one is interested in shifting the positions of only the dominant eigenvalues. In these situations it is not necessary that the system be completely controllable to achieve this objective; however, it is necessary that the eigenvalues in question be controllable [5]. In many situations it is possible to affect a shift of the dominant eigenvalues with the modal methods to obtain better system behaviour with incomplete state feedback [6,7], whereas incomplete state feedback cannot be considered directly in the earlier technique. Furthermore, the modal control method of design is simple and straightforward. It is thus apparent that the modal control approach offers advantages over the method of design, using optimal control theory, adopted by Yu et al.

CHAPTER 2

MODAL CONTROL APPROACH

2.1 Modal Control Theory and Methods

Assuming that the eigenvalues of the system represented by eqn.(1) are distinct, the time response of the system with zero control inputs in terms of the system modes is given by

$$\underline{x}(t) = \sum_{i=1}^{n} c_i \, \underline{U}^i \exp(\lambda_i t) \qquad (6)$$

where λ_i and $\underline{U}^i$, $(i = 1,2,\ldots,n)$ are the eigenvalues and eigenvectors respectively of the uncontrolled system matrix A, c_i's are appropriate constants, and the term $\underline{U}^i \exp(\lambda_i t)$ represents the mode of the system associated with eigenvalue λ_i. It is observed that the speed of response of the system is determined by the real parts of the eigenvalues of the system and the oscillatory nature is characterised by the imaginary parts of the eigenvalues. So, by shifting both the real and imaginary parts of the eigenvalues of the system to appropriate new locations in the left half of the complex plane, an initially unstable mode can be made stable or the time constant of any stable mode can be reduced to the extent desired and improve the overall transient response of the system.

Now, for the system defined by eqn.(1), it is possible to shift any specified eigenvalues to any assigned new locations by linear state feedback (with the constraint that complex eigenvalues should occur in conjugate pairs) if the corresponding modes are controllable [4,5]. When a particular eigenvalue, say λ_i, is to be shifted to a preassigned location, the corresponding eigenvector $\underline{V}^i$ of matrix A' is to be used as measurement vector and the resulting output signal is to be amplified by the appropriate amount before being fedback. Thus when ℓ ($\leq n$) of the eigenvalues of the system (1) are modified, the resulting closed-loop system will have ℓ new eigenvalues and ℓ new corresponding eigenvectors and the rest $(n-\ell)$ eigenvalues and their corresponding eigenvectors remain unchanged [2,3,4,5]. A proof of this is provided in Appendix A.

Thus by using modal control method of approach any number of eigenvalues of the system (1) can be shifted to some pre-assigned locations without affecting the other eigenvalues in order to stabilize an initially unstable system or to improve the transient behaviour of an initially stable system, or both, provided that these modes are controllable and all the state variables are available for feedback.

Various modal control methods are discussed by Porter et al [2,3,4,5] for shifting the real as well as complex eigenvalues of a system represented by eqn.(1). Making use of these methods linear complete state feedback loops can be designed so that the closed-loop system can have the preassigned choice of eigenvalues. The detailed discussion of one of modal control methods that has been used in this work is presented in Appendix B.

2.2 Sector Criterion

It is essential that the eigenvalues of the closed-loop system are to be preassigned before the eigenvalues of the uncontrolled system are shifted to these new locations by using modal control methods. For the preassignment of the new locations of eigenvalues, a sector criterion is used which is based on the fundamental concept of damping ratio, ξ and undamped natural frequency, w_n, as explained in Figure 1.

If the dominant eigenvalues of the system that are to be shifted happen to be a complex conjugate pair, then a desired degree of damping ratio, ξ and undamped natural frequency, w_n can be prescribed and the new locations for the conjugate pair can be determined. If another pair of complex conjugate eigenvalues is to be shifted, then ξ and w_n for this pair are chosen such that the sector defined by these ξ and w_n values is contained within the sector defined for the first dominant conjugate pair and the new

locations for the second pair are placed to the left of those preassigned for the first pair. In case a real eigenvalue is to be shifted, then the new location for that real eigenvalue can be chosen arbitrarily such that it lies to the left of the first complex conjugate pair.

Making use of the above sector criterion procedure the new locations for those eigenvalues of the uncontrolled system that are to be shifted, can be preassigned. However, after shifting the eigenvalues to the prescribed new locations, if the resulting feedback gains are high, then the choice of preassigned locations is to be suitably modified.

2.3 Choice of Input Variables

When a number of eigenvalues of the system (1) are to be shifted, and if the control variables that can be manipulated are many, then the choice of the control input to be used for shifting a particular eigenvalue can be determined by observing the terms $\underline{V}^{i'}\underline{b}_j$, $(j = 1,2,\ldots, r)$, r being the number of control inputs and $\underline{V}^i$ being the eigenvector of matrix A' corresponding to the eigenvalue λ_i that is to be shifted [6,7]. The inability of a particular input say j-th input, to excite the i-thmode is indicated by the relationship

$$\underline{V}^{i'}\ \underline{b}_k \quad = 0 \qquad (7)$$

Thus, it is clear that there may be more than one control input which can excite a particular mode. In such a case, a good choice can be to select that control input for which the $\underline{v}^{i'} \underline{b}_j$ term has absolute maximum value among all such terms which refer to different control inputs that can excite the same mode [6,7]. A different choice may lead to a higher feedback gain requirement. It is also possible that a particular eigenvalue cannot be shifted using any of the r available control inputs ; in such a case the corresponding mode is said to be uncontrollable.

2.4 Possibility of Incomplete State Feedback

Upto now it has been assumed that all the state variables should be available for linear feedback in order to shift the eigenvalues of the uncontrolled system to some specified new locations. But in many practical situations all the states cannot be measured, and even if they could be, it may be uneconomical to measure all of them. In such situations it may be possible to use incomplete state linear feedback for shifting the eigenvalues by modal control methods. A design technique has been discussed by Davison et al [6,7] for shifting the dominant real eigenvalues of a linear time-invariant system with incomplete state feedback. A similar technique, the details of which are given in Appendix C, has been used in

this work for shifting both real and complex eigenvalues of the power system under consideration. By using this method certain unmeasurable state variables as well as certain measurable states may be eliminated from the linear feedback and at the same time achieve the proper locationing of the eigenvalues of the closed-loop system for better dynamic behaviour of the system.

However, it is to be noted that when some of the eigenvalues (k) of the open-loop system are shifted to pre-assigned locations using incomplete state feedback, the resulting closed-loop system may not have the remaining (n-k) eigenvalues unchanged unlike in the case of complete state feedback. The manner in which these remaining eigenvalues get affected has not yet properly been established. Hence, it is necessary to check the eigenvalue locations of the closed-loop system after the design and establish that the design is satisfactory only when the eigenvalues which are not considered for shifting, are not modified to a large extent.

2.5 Advantages of Modal Control Approach

Modal control approach can be found to be advantageous over the method that uses the optimal control theory (as used by Yu et al). Computationally the modal control method involves mainly determination of eigenvalues and eigenvectors, whereas in the latter method an algebraic matrix Riccati equation is to be

solved using iterative techniques. Furthermore, number of designs in an iterative manner are to be done in the latter case for obtaining a desired degree of transient response of the system, whereas in the former case such iterative procedures are not necessary. The modal control method is simple and straightforward. It gives more insight into the controlling of the system; that is the control configuration designed indicates which of the input variables to manipulate for control and which are the state variables that can be used for linear incomplete state feedback. These advantages become significant when the order of the system is large and the input variables that can be manipulated are many. Since an implicit control can be exercised over the location of the eigenvalues of the closed-loop system in the modal control method; any desired degree of improvement in the dynamic behaviour of the system can be achieved, of course subject to the engineering constraints, like gain limitations.

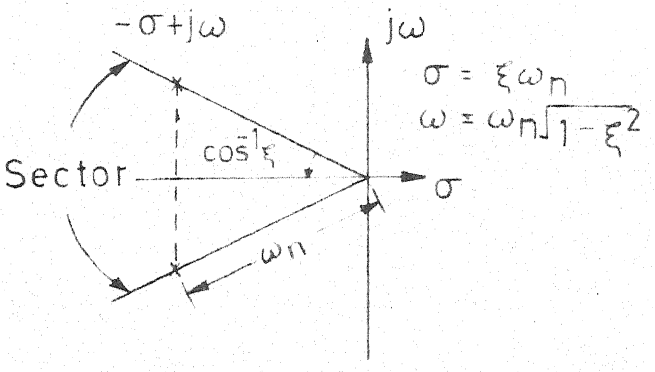

FIG. 1 SECTOR DEFINITION

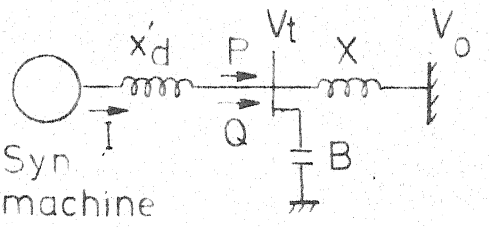

FIG.2 SYNCHRONOUS MACHINE INFINITE BUS SYSTEM

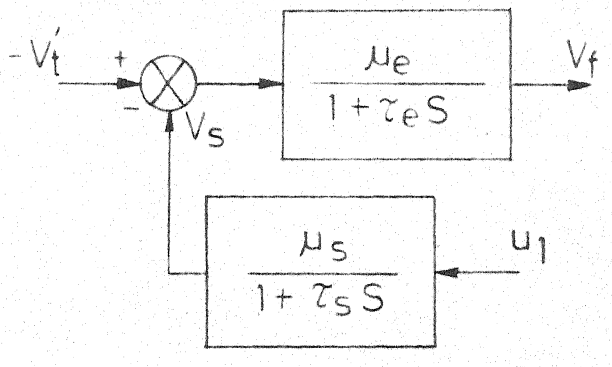

FIG. 3 EXCITER-VOLTAGE REGULATOR SYSTEM

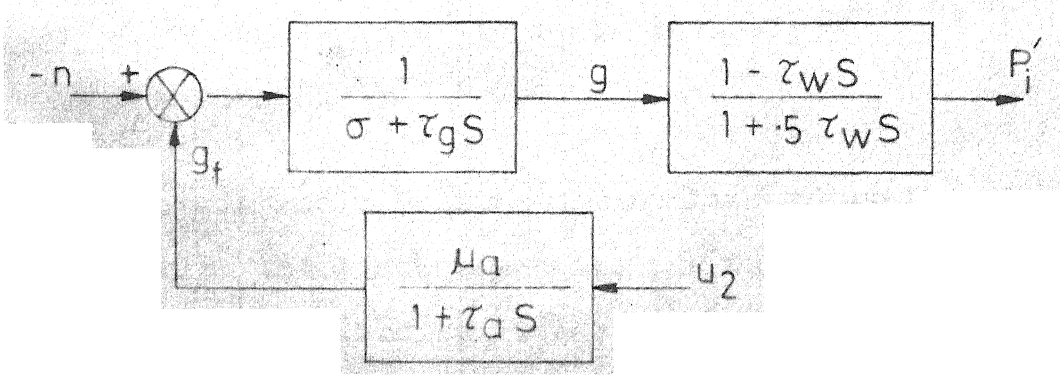

FIG. 4 GOVERNOR-HYDRAULIC SYSTEM

CHAPTER 3

APPLICATION OF MODAL CONTROL APPROACH TO THE POWER SYSTEM

3.1 System Model

The power system whose dynamic behaviour is to be improved by a feedback control law consists of a synchronous generator driven by a hydraulic turbine, having an exciter-voltage regulator and a turbine speed-governor as given in Figures 2,3 and 4. The system was considered by Yu et al[1] for which they obtained a feedback control law using the linear optimal regulator theory for quadratic performance index as defined by eqn.(2). The optimal controller is designed with the choice of the following Q and R matrices.

$$Q = \text{diag}\,[10 \quad 10 \quad 1 \quad 1 \quad 1 \quad 1 \quad 1 \quad 1]$$
$$R = \text{diag}\,[1 \quad 1] \qquad (8)$$

Appendix D gives the nonlinear equations which describe the system dynamics, as well as the linearized equations derived by linearizing the nonlinear equations at an operating point. The linearised equations obtained in this manner are

$$\dot{\underline{x}}(\tau) = A\,\underline{x}(\tau) + B\,\underline{u}(\tau) \qquad (9)$$

where the state vector

$$\underline{x}(\tau) = [\delta \quad n \quad \psi_f \quad v_f \quad v_s \quad g \quad g_f \quad h]' \qquad (10)$$

I.I.T. KANPUR
CENTRAL LIBRARY
Acc. No. A 28387

The A and B matrices are given by

$$A = \begin{bmatrix} 0.0 & 1.0 & 0.0 & 0.0 & 0.0 & 0.0 & 0.0 & 0.0 \\ -0.6830 & -0.0346 & -0.0816 & 0.0 & 0.0 & 0.8820 & 0.0 & 1.320 \\ -0.0832 & 0.0 & -0.0254 & 0.1370 & 0.0 & 0.0 & 0.0 & 0.0 \\ -0.1300 & 0.0 & -0.1070 & -0.1370 & -1.3700 & 0.0 & 0.0 & 0.0 \\ 0.0 & 0.0 & 0.0 & 0.0 & -0.2740 & 0.0 & 0.0 & 0.0 \\ 0.0 & -0.0265 & 0.0 & 0.0 & 0.0 & -0.0616 & -1.3700 & 0.0 \\ 0.0 & 0.0 & 0.0 & 0.0 & 0.0 & 0.0 & -13.700 & 0.0 \\ 0.0 & 0.0531 & 0.0 & 0.0 & 0.0 & 0.1230 & 2.7400 & -0.1710 \end{bmatrix} \quad (11)$$

$$B = \begin{bmatrix} 0 & 0 & 0 & 0 & 1 & 0 & 0 & 0 \\ 0 & 0 & 0 & 0 & 0 & 0 & 1 & 0 \end{bmatrix}^T \quad (12)$$

The control vector is given by

$$\underline{u}(\tau) = [u_v \quad u_g]' \tag{13}$$

where

$$u_v \triangleq \frac{\mu_s u_1}{\beta \tau_s} \quad ; \quad u_g \triangleq \frac{\mu_a u_2}{\beta \tau_a} \tag{14}$$

The variable τ in eqn.(9) is scaled time and is related to the real time t by the equation

$$\tau = 7.308\ t \tag{15}$$

3.2 Location of Modal Control Configurations with Complete State Feedback

The eigenvalues of the uncontrolled power system (9) and the corresponding eigenvectors of A' are determined [8], which are given in Table 1. From the eigenvalue locations it can be inferred that the transient response of the system is highly unsatisfactory. Indeed it is observed from the transient response curves given in figures 5 to 12, that the transient response to a given initial condition of the uncontrolled system is quite oscillatory and it takes considerable time for the system to settle down to steady state. In order to improve the transient behaviour of the power system the five dominant eigenvalues of the uncontrolled system consisting of two complex pairs and one real eigenvalue, can be shifted to some appropriate locations in the complex plane.

Table 1: Eigenvalues and Eigenvectors of [illegible] Power System.

S. No.	Eigenvalues	Eigenvectors of A' for five dominant eigenvalues		
		1,2	3	4,5
1	-0.0114 $\pm$j0.7986	$-5.1533\times10^{-1}\pm j1.0411\times10^{-1}$	-2.5151×10^{-2}	$1.5821\times10^{-2}\mp j4.0751\times10^{-3}$
2		$1.2091\times10^{-1}\pm j6.0500\times10^{-1}$	-1.8973×10^{-3}	$-2.7125\times10^{-2}\pm j5.1386\times10^{-5}$
3	-0.0572	$-6.3479\times10^{-2}\pm j1.1270\times10^{-2}$	1.0192×10^{-3}	$7.2614\times10^{-3}\mp j1.5671\times10^{-1}$
4	-0.0772 $\pm$j0.1146	$2.1537\times10^{-4}\pm j1.0924\times10^{-2}$	1.7499×10^{-3}	$-1.4366\times10^{-1}\mp j8.3658\times10^{-2}$
5		$-1.7021\times10^{-2}\mp j5.2275\times10^{-3}$	-1.1059×10^{-2}	$1.0 \quad \mp j0.0$
6	-0.1952	$6.8356\times10^{-1}\mp j2.4459\times10^{-1}$	-9.9481×10^{-1}	$2.4755\times10^{-1}\pm j3.3903\times10^{-1}$
7	-0.2740	$1.3273\times10^{-1}\pm j1.6736\times10^{-2}$	9.5478×10^{-2}	$-5.5587\times10^{-2}\pm j4.0549\times10^{-3}$
8	-13.700	$1.0 \quad \mp j0.0$	-2.2007×10^{-2}	$-1.5277\times10^{-1}\pm j1.8735\times10^{-1}$

According to the procedure outlined in Section 2.3, the choice of the control inputs to shift the five dominant eigenvalues is determined after examining the terms $\underline{v}^{i'}\ \underline{b}_j$, (i = 1,2,...,n and j = 1,2). These terms are given in Table 2. It is found that both the control variables can excite all the five modes, but a good choice is that the u_g control input is to be used for shifting the first three dominant eigenvalues and the u_v control input is to be used for shifting the other two eigenvalues. Different modal control cinfigurations are designed after preassigning the new locations for these five eigenvalues. These are given below.

Modal control configuration 1

For the first dominant pair of complex eigenvalues, with the specifications of $\xi = 0.4$ and $w_n = 1.0$, the new locations are determined to be $-0.4 \pm j0.915$, in accordance with the sector criterion (Section 2.2). Then for the second dominant pair the new locations are taken to be $-0.96 \pm j0.72$, this corresponds to $\xi = 0.8$ and $w_n = 1.2$. The new location for the real eigenvalue is arbitrarily chosen to be -0.6.

Using the modal control method outlined in Appendix B, the first three eigenvalues consisting of first dominant conjugate pair and one real eigenvalue, are shifted simultaneously using u_g control. Then the

second dominant pair of complex eigenvalues is shifted using u_v control. The resulting feedback gain vectors are given in Table 4 and the final eigenvalue locations are given in Table 5.

Modal control configuration 2

For this configuration, the new locations for the five dominant eigenvalues of the uncontrolled system are chosen to lie farther to the left in the complex plane, than the corresponding locations chosen for configuration 1 in order to see how the feedback gains get affected. The preassigned choice for the new locations along with the ζ and w_n specifications, is given in Table 3. The shifting of the five eigenvalues is then carried out in the same order as it is done in the design of the configuration 1. The resulting feedback gain vectors are given in Table 4 and the closed-loop system eigenvalues in Table 5.

Modal control configuration 3

This configuration is designed to show that the shifting of the first three dominant eigenvalues, very much farther to the left in the complex plane, results in high feedback gain requirements for the u_g control. The preassigned choice of new locations is given in Table 3 and the resulting gain vector after shifting the three eigenvalues is given in Table 4.

Table 2: $\underline{v}^{i'}\underline{b}_j$, (i=1,2,...,n; j=1,2) terms

Term	Value
$\underline{v}^{1'}\underline{b}_1$	$-1.7021\times10^{-2}\mp j5.2275\times10^{-3}$
$\underline{v}^{2'}\underline{b}_1$	
$\underline{v}^{1'}\underline{b}_2$	$1.3273\times10^{-1}\pm j1.6736\times10^{-2}$
$\underline{v}^{2'}\underline{b}_2$	
$\underline{v}^{3'}\underline{b}_1$	-1.1059×10^{-2}
$\underline{v}^{3'}\underline{b}_2$	9.5478×10^{-2}
$\underline{v}^{4'}\underline{b}_1$	$1.0\mp j0.0$
$\underline{v}^{5'}\underline{b}_1$	
$\underline{v}^{4'}\underline{b}_2$	$-5.5587\times10^{-2}\pm j4.0549\times10^{-3}$
$\underline{v}^{5'}\underline{b}_2$	

Table 3: Preassignment of New Locations for the Five Dominant Eigenvalues.

S. No.	Modal Control Configuration 1	2	3	4
1	$-0.40\pm j0.9150$ ($\xi=0.4, w_n=1.0$)	$-0.60\pm j0.8000$ ($\xi=0.6, w_n=1.0$)	$-1.20\pm j1.6000$ ($\xi=0.6, w_n=2.0$)	$-0.40\pm j0.9150$
2				
3	-0.60	-0.80	-0.60	-0.60
4	$-0.96\pm j0.7200$ ($\xi=0.8, w_n=1.2$)	$-1.08\pm j0.5230$ ($\xi=0.9, w_n=1.2$)	$-0.96\pm j0.7200$	$-1.80\pm j0.8718$ ($\xi=0.9, w_n=2.0$
5				

Table 4: Feedback Gain Vectors

Optimal Controller[1]		Modal Control Configurations							
		1		2		3		4	5
$-\underline{G}_v$	$-\underline{G}_g$	$\underline{G}_v$	$\underline{G}_g$	$\underline{G}_v$	$\underline{G}_g$	$\underline{G}_v$	$\underline{G}_g$	$\underline{G}_v$	$\underline{G}_v$
-0.3313	-1.1545	0.4812	0.8812	0.5708	1.4505	0.6284	-7.9352	1.3822	-1.2396
-0.1065	4.6784	0.1840	-5.0268	0.2298	-7.9841	-0.1948	-25.4274	0.4687	38.2124
-0.8016	-0.3098	1.8181	0.0857	1.8014	0.1510	1.8366	-1.0508	5.2688	0.0538
-0.9763	0.0023	1.2038	-0.1003	1.2259	-0.1551	1.9991	-0.5366	3.2423	0.7986
1.6619	-0.0214	-1.7656	0.1831	-2.0056	0.2760	-1.7656	0.4686	-3.4456	-1.3200
3.0856	-1.6837	-6.5651	8.3796	-6.4963	11.0682	-6.5982	50.5043	-19.467	-80.169
-0.0214	1.1581	0.0933	-1.3200	0.0693	-1.9200	0.0228	-2.9200	0.2667	9.5009
1.4128	5.0112	-2.7737	-2.6776	-2.8549	-4.4920	-3.1615	8.9852	-8.2778	9.5746

Table 5: Eigenvalues of Closed-Loop System

S. No.	Uncontrolled system	Controlled System: Optimum controller	Modal Controllers 1	2	3	4
1	-0.0114	-0.0838	-0.1952	-0.1952	-0.1952	-0.1952
2	±j0.7986	-0.1443	-0.2740	-0.2740	-0.2740	-0.2740
3	-0.0572	-0.3771 ±j0.9478	-0.4000 ±j0.9150	-0.6000 ±0.8000	-1.2000 ±j1.6000	-0.4000 ±j0.9150
4	-0.0772 ±j0.1142					
5		-0.5679	-0.6000	-0.8000	-0.6000	-0.6000
6	-0.1952	-0.9696 ±j0.6473	-0.9600 ±j0.7200	-1.0800 ±j0.5230	-0.9600 ±j0.7200	-1.8000 ±j0.8718
7	-0.2740					
8	-13.7000	-13.7344	-13.7000	-13.7000	-13.7000	-13.7000

Modal control configuration 4

This configuration is designed to show that the shifting of the second dominant pair of complex eigenvalues, very much farther to the left in the complex plane, requires high feedback gain. The preassigned locations are given in Table 3 and the resulting gain vectors after shifting are given in Table 4.

Modal control configuration 5

This configuration is designed to show that a wrong choice of control input for shifting a particular eigenvalue may lead to high feedback gain requirements. For shifting the first three dominant eigenvalues using of u_v control variable is not a good choice. So, using u_v control the three dominant eigenvalues are shifted simultaneously. The resulting feedback gain vector is given in Table 4. The preassigned locations are the same as specified in configuration 1.

The transient response characteristics of the power system with modal control configurations 1 and 2 that use complete state feedback are obtained as shown in Figures 5 to 12. Standard 4-th order Runge-Kutta method is used for solving the differential equations of the system to obtain the transient responses. The initial conditions used are those considered by Yu et al [1] which were found from the release of a

load perturbation P_e'. The transient response for the uncontrolled system as well as for the controlled system with optimal controller (designed by Yu et al.) are also obtained for the given initial conditions.

3.3 Design of Modal Control Configurations with Incomplete State Feedback.

It has been decided here also to shift the five dominant eigenvalues of the uncontrolled system by designing modal control loops with incomplete state feedback. The preassigned new locations for the five dominant eigenvalues are considered to be the same as those used in designing the modal control configuration 1 with complete state feedback. The order of shifting considered is also the same as followed earlier i.e., the first three dominant eigenvalues are shifted in the beginning using u_g control and then the other two eigenvalues are shifted using u_v control input.

According to the procedure outlined in Appendix C, first the average steady state values of the uncontrolled system are determined with both the control inputs applied in step function manner [6]. Here equation (C.4) is used. These average steady state values are given in Table 6. Since the first three dominant eigenvalues are to be considered first for shifting, the eigenvectors of A' corresponding to these three eigenvalues are modified

using the eqn.(C.5). Examining the three new eigenvectors (given in Table 7), it is found that the 2nd, 8th, 7th, 4th and 5th elements in each new eigenvector, are the smallest, in that order. Since n is already used as feedback signal in the original system (Figure 4), the other four states i.e., h, g_f, v_f and v_s may be excluded from feedback.

Modal control configurations 6,7,8,9 and 10 with incomplete state feedback excluding one (h), two (h and g_f), three (h, g_f and v_s) and(h, g_f and v_f) and four (h, g_f, v_f and v_s) states respectively are successfully designed which effectively control the first three dominant modes of the uncontrolled system. The details of the eigenvalue location for the resulting closed-loop systems and the gain vectors are given in Tables 8 to 12.

Since it has been decided earlier to shift all the five dominant eigenvalues, the second dominant conjugate pair is then shifted using u_v control following the same procedure as outlined in Appendix C. However, in this case the appropriate closed-loop system resulting after shifting the first three eigenvalues with incomplete state feedback is to be considered as a starting point. Two modal control configurations 6,7 are successfully designed with incomplete state feedback dropping one (h) and two (h,g_f) states respectively, which effectively

control the five modes of the uncontrolled system. Design of modal control loops excluding three and four states from feedback are not successful. The details of the gain vectors and the eigenvalue locations for the closed-loop systems for these controllers 6 to 10 are given in Tables 8 to 12.

The transient response characteristics for the modal controlled system with incomplete state feedback dropping two states are obtained, as given in Figures 5 to 12.

3.4 Discussion of Results

Examination of the gain vectors for various modal control configurations given in Table 4, indicates that in general farther the locations to the left in the complex plane to which the eigenvalues are to be shifted, the more is the feedback gain required. Furthermore, we cannot shift the eigenvalues to any large extent because of the feedback gain limitations, which is necessary to consider from the practical implementation point of view. It is also clear from the design of modal control configuration 5, that only a proper choice of control input for shifting various eigenvalues can give rise to lower feedback gain requirements.

The transient response curves for the modal controlled power system with complete state feedback

as well as incomplete state feedback, as given in Figures 5 to 12, compare well with that of the system with optimal controller designed earlier [1]. In fact the response of the modal controlled system with complete state feedback is better than that of the optimal controlled system designed by Yu et al [1].

Table 6: $\underline{X}^{ss}$ - Average Steady State of the System with both Inputs given in Step Function Manner.

S.No.	State	Value
1	δ	1.1605
2	n	0.0
3	ψ_f	-18.4720
4	v_f	-2.7199
5	v_s	1.8248
6	g	-0.8117
7	g_f	0.0365
8	h	0.0010

Table 7: Modified Eigenvectors for the First Three Dominant Eigenvalues.

S.No.	$\underline{V}^1$, $\underline{V}^2$	$\underline{V}^3$
1	$-0.5981 \pm j0.1208$	-0.0292
2	$0.0 \quad \pm j0.0$	0.0
3	$1.1730 \mp j0.2082$	-0.0188
4	$-0.0006 \mp j0.0297$	-0.0048
5	$-0.0311 \mp j0.0095$	-0.0202
6	$-0.5548 \pm j0.1985$	0.8075
7	$0.0048 \pm j0.0006$	0.0035
8	$0.0010 \pm j0.0$	-0.00002

Table 8: Modal Controller with Incomplete State Feedback excluding 'h' state (configuration 6)

Shifting of first three dominant eigenvalues		Shifting the next two dominant eigenvalues	
Gain Vector $\underline{G}_g$	Resulting Closed-loop System Eigenvalues	Gain Vector $\underline{G}_v$	Resulting Closed-loop System Eigenvalues
0.8812	-0.0771±j0.1140	0.4396	-0.1610±j0.2370
-5.0268		0.2231	
0.0857	-0.1613±j0.2366	1.8100	-0.2749
-0.1003		1.2035	-0.3411±j1.1207
0.1831	-0.2740	-1.7658	
8.3796	-0.3497±j1.1206	-2.4492	-0.9695±j0.7068
-1.3200		0.0877	
0.0	-14.2734	0.0	-14.2714

Table 9: Modal Controller with Incomplete State Feedback excluding 'h', 'g_f' states (configuration 7)

Shifting of first three dominant eigenvalues		Shifting of the next two dominant eigenvalues	
Gain Vector $\underline{G}_g$	Resulting Closed-loop System Eigenvalues	Gain Vector $\underline{G}_v$	Resulting Closed-loop system eigenvalues
0.8812	-0.0771±j0.1140	0.4347	-0.1614±j0.2432
-5.0268		0.2216	
0.0857	-0.1616±j0.2428	1.8089	-0.2750
-0.1003		1.2033	-0.3761±j1.1458
0.1831	-0.2740	-1.7659	
8.3796	-0.3862±j1.1464	-2.3351	-0.9719±j0.7056
0.0		0.0	
0.0	-12.8799	0.0	-12.8758

Table 1C: Modal Controller with Incomplete State Feedback excluding 'h', 'g_f', 'v_f' states (configuration 9)

Shifting of first three dominant eigenvalues		Shifting of the next two dominant eigenvalues	
Gain Vector $\underline{G}_g$	Resulting Closed-loop System Eigenvalues	Gain Vector $\underline{G}_v$	Resulting Closed-loop system eigenvalues
0.8812	-0.0783±j0.1170	0.4300	-0.0408±j0.4134
-5.0268		0.2345	
0.0857	-0.1607±j0.2367	1.7148	-0.1507±j0.2426
0.0		0.0	
0.1831	-0.2740	-1.7634	-0.3827±j1.1463
8.3796	-0.3858± j1.1472	-2.1336	
0.0		0.0	-2.1426
0.0	-12.8799	0.0	-12.8758

Table 11: Modal Controller with Incomplete State Feedback excluding 'h', 'g_f','v_s' at the Reconfiguration B)

Shifting of first three dominant eigenvalues		Shifting of the next two dominant eigenvalues	
Gain Vector $\underline{G}_g$	Resulting Closed-loop System Eigenvalues	Gain Vector $\underline{G}_v$	Resulting Closed-loop System Eigenvalues
0.8812	-0.0771±j0.1140	0.4367	-0.1023±j1.2655
-5.0268		0.2193	
0.0857	-0.1616±j0.2428	1.8106	-0.1602±j0.2430
-0.1003		1.1918	
0.0	-0.2740	0.0	-0.2185
8.3796	-0.3862±j1.1464	-2.3842	-0.3900±j1.1639
0.0		0.0	
0.0	-12.8799	0.0	-12. 8801

Table 12: Modal Controller with Incomplete State Feedback excluding 'h', 'ϵ_f', 'v_s', 'v_f' state variable information [illegible]

Shifting of first three dominant eigenvalues		Shifting of the next two dominant eigenvalues	
Gain Vector $\underline{G}_g$	Resulting Closed-loop System Eigenvalues	Gain Vector $\underline{G}_v$	‡ Resulting Closed-loop System Eigenvalues
0.8812	-0.0783±j0.1170	0.4321	0.1987±j0.5971
-5.0268		0.2322	
0.0857	-0.1607±j0.2367	1.7167	-0.1527±j0.2416
0.0		0.0	
0.0	-0.2740	0.0	-0.3879±j1.1482
8.3796	-0.3858±j1.1472	-2.1840	
0.0		0.0	-0.8799
0.0	-12.8799	0.0	-12.8799

‡ System is unstable.

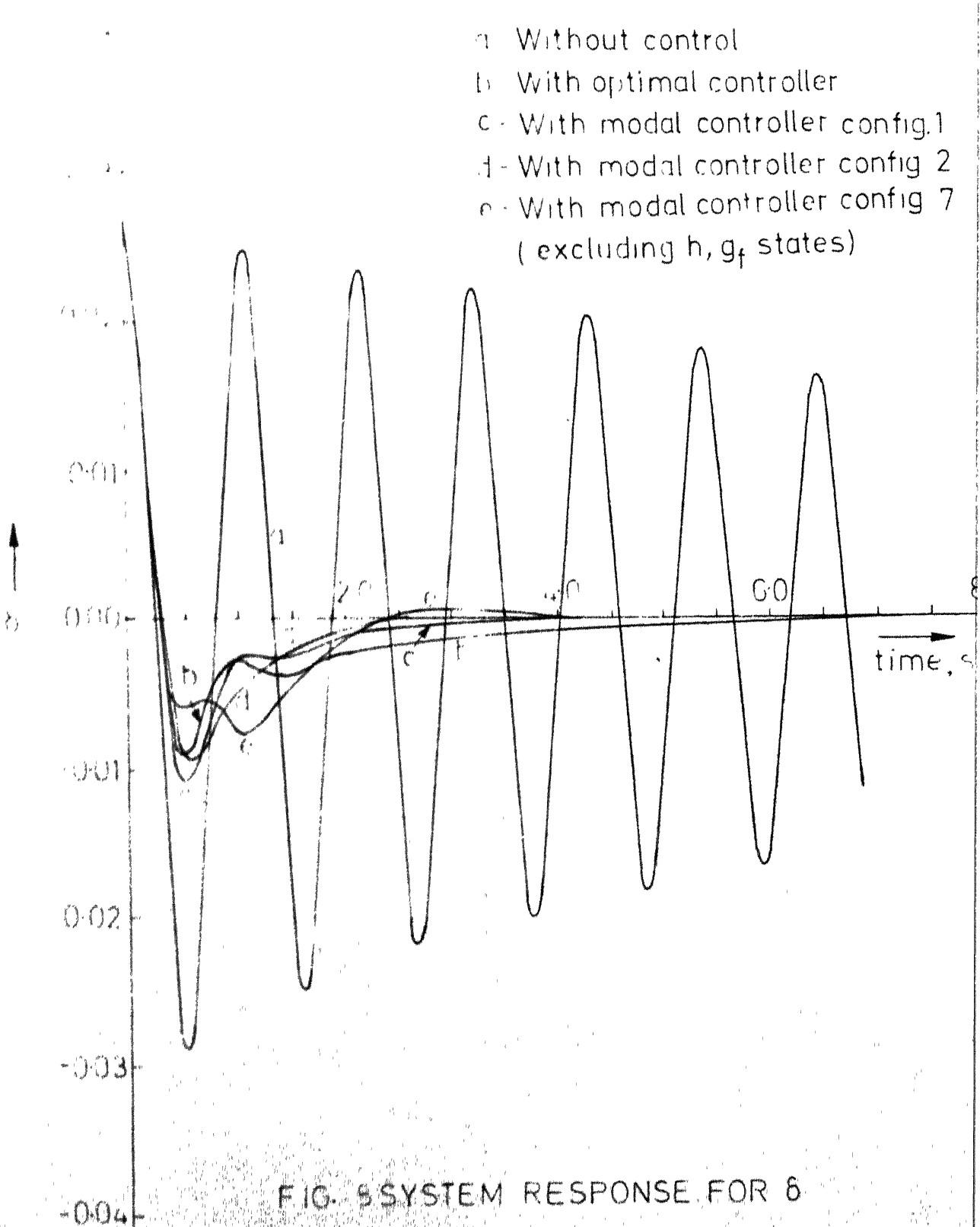

FIG. 8 SYSTEM RESPONSE FOR δ

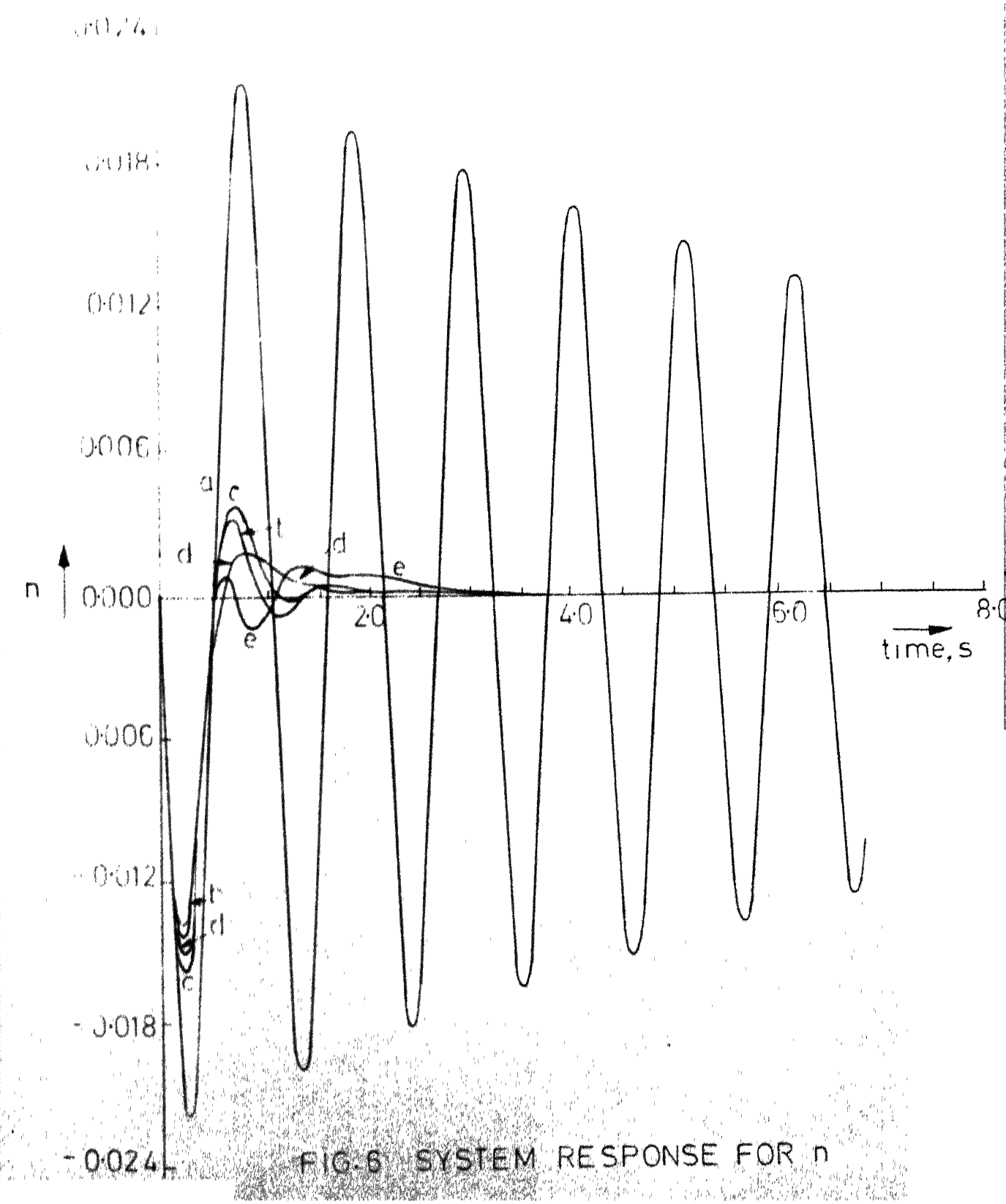

FIG. 6 SYSTEM RESPONSE FOR n

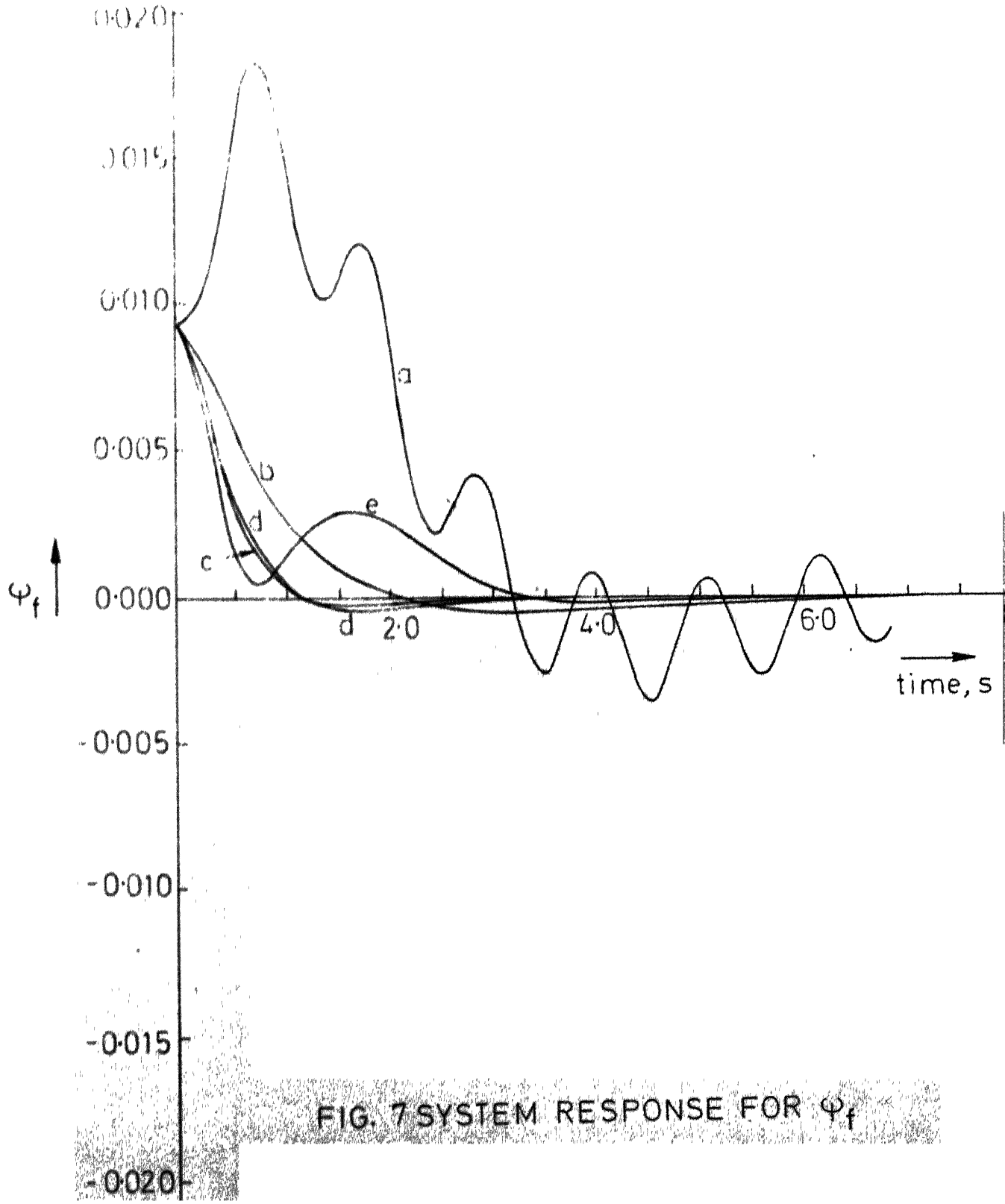

FIG. 7 SYSTEM RESPONSE FOR Ψ_f

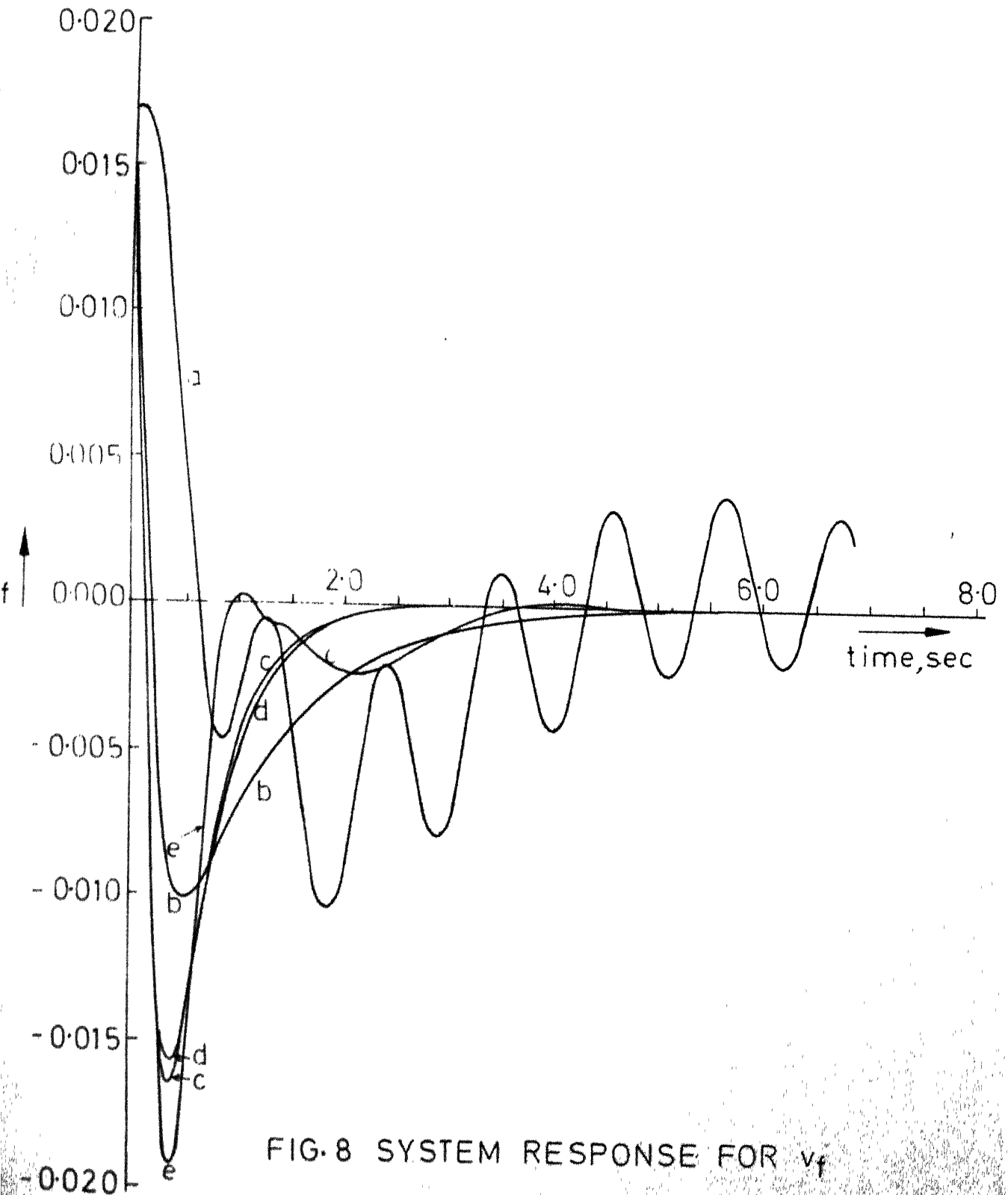

FIG. 8 SYSTEM RESPONSE FOR v_f

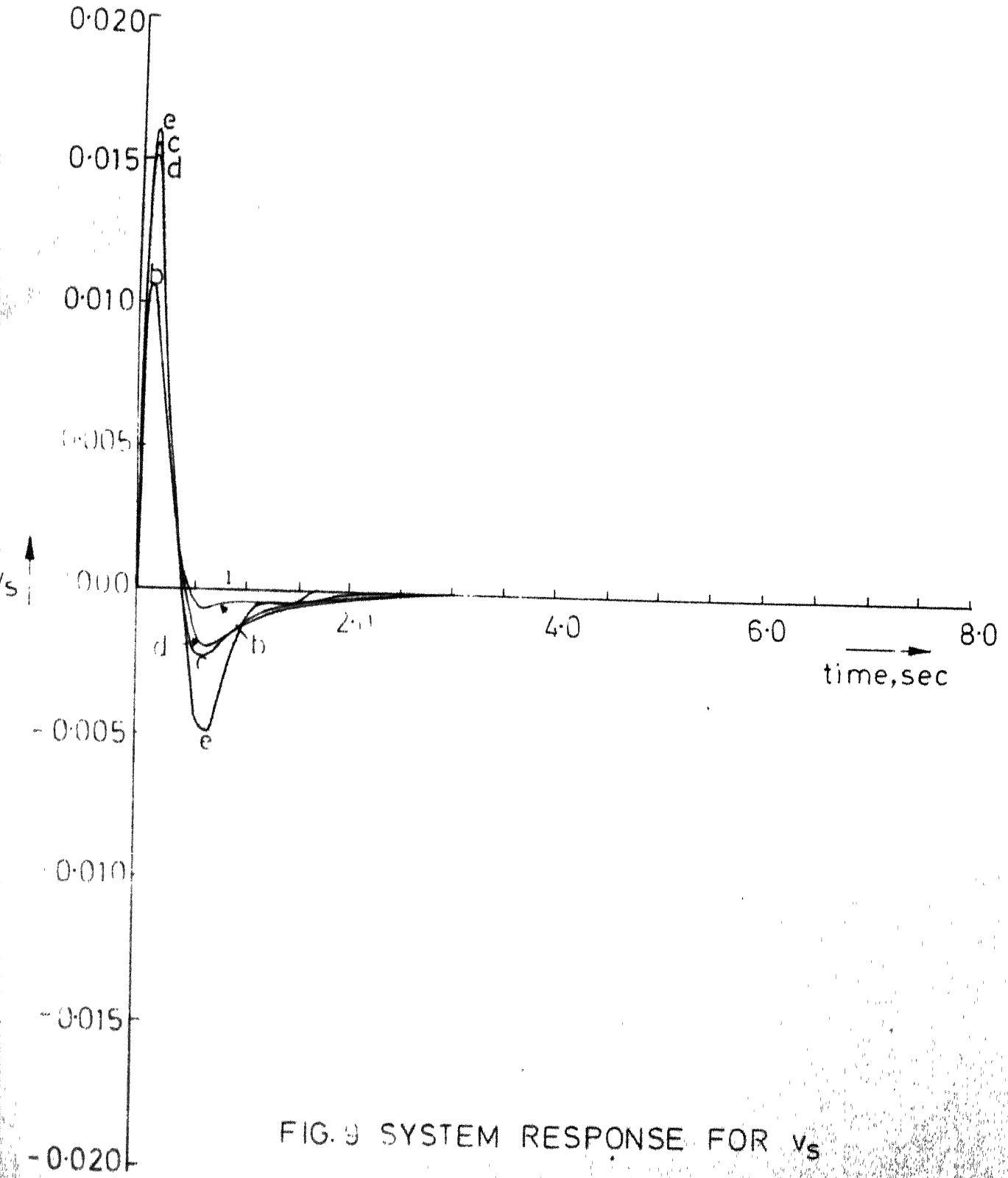

FIG. 9 SYSTEM RESPONSE FOR v_s

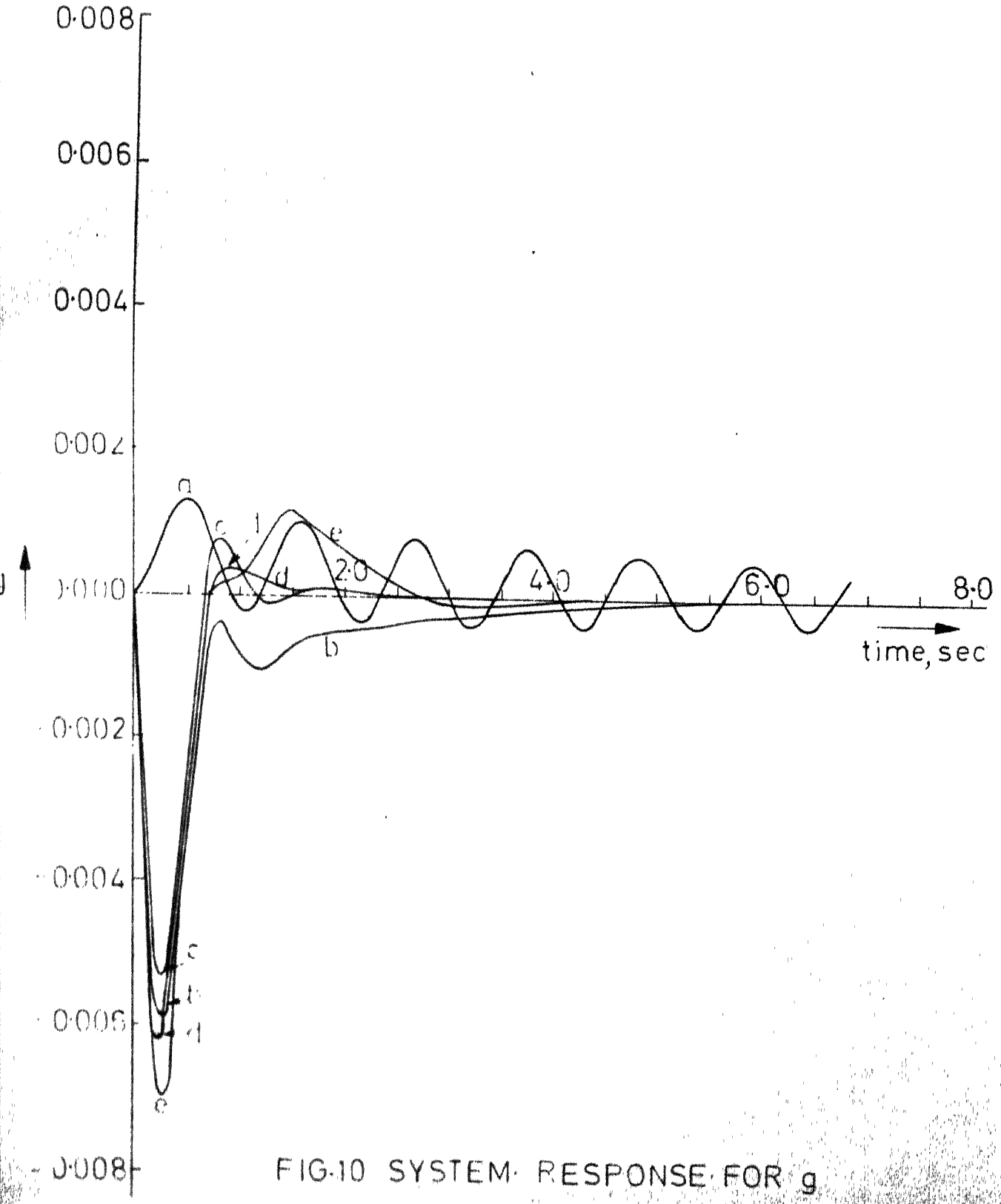

FIG·10 SYSTEM· RESPONSE· FOR g

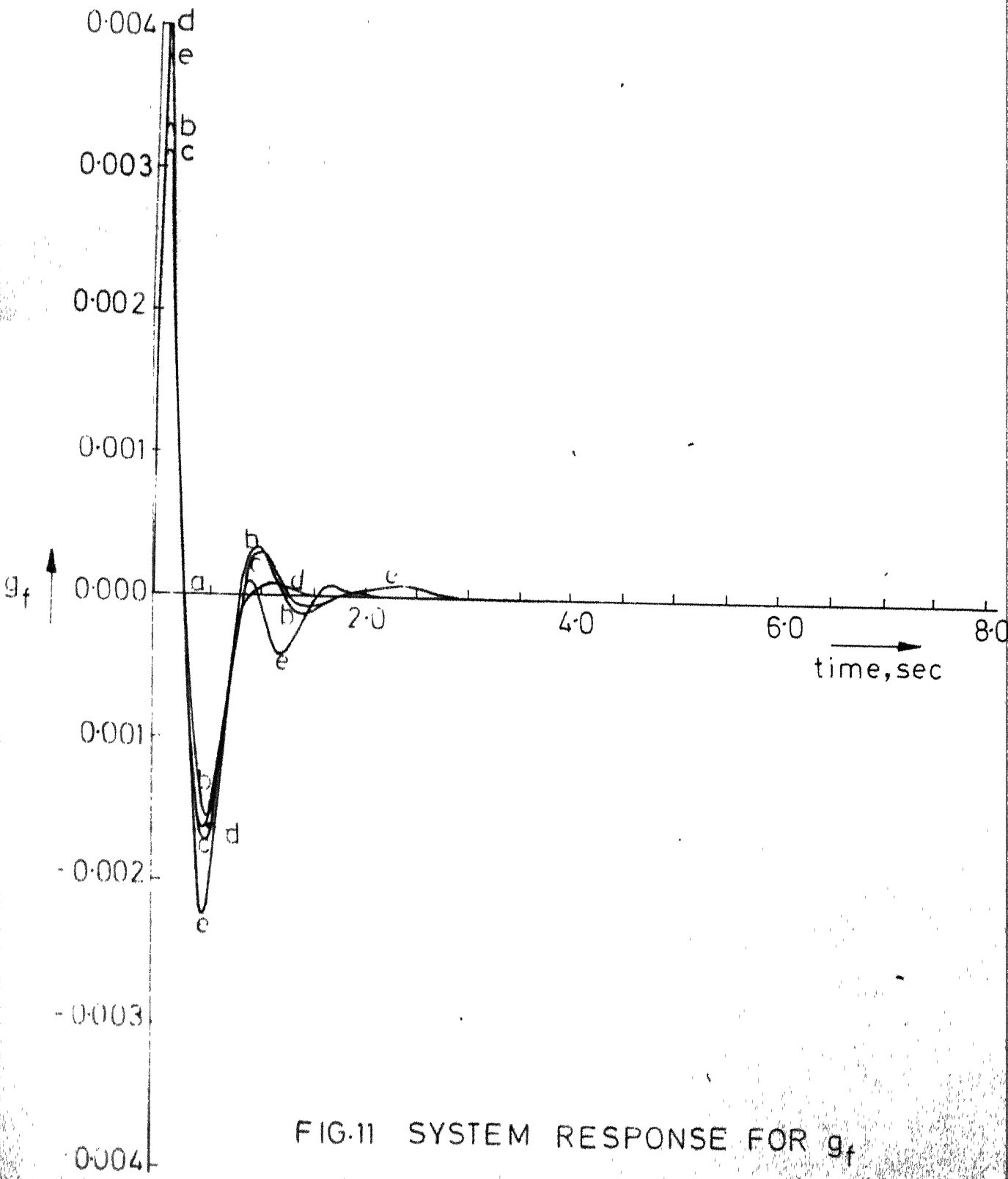

FIG·11 SYSTEM RESPONSE FOR g_f

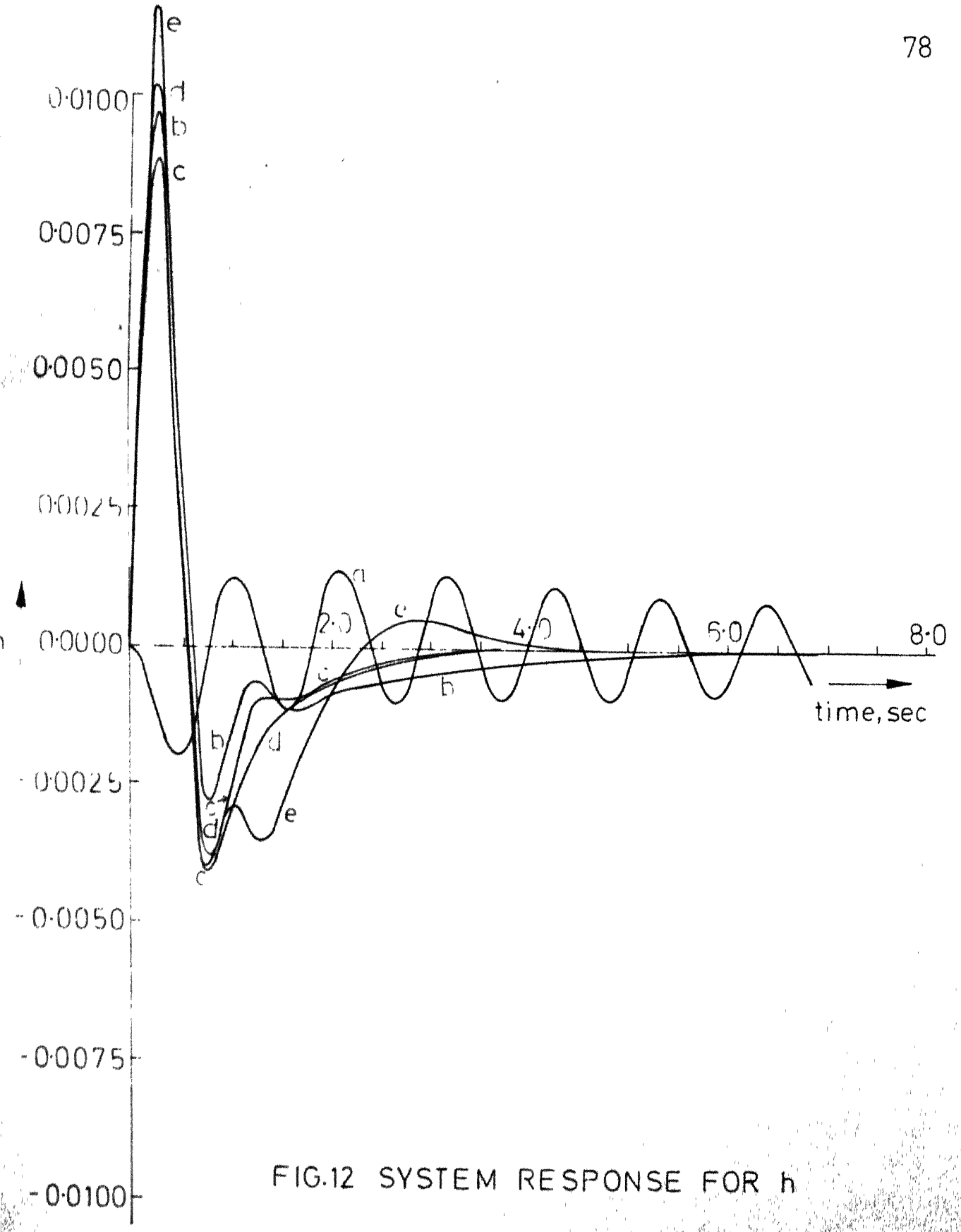

FIG.12 SYSTEM RESPONSE FOR h

CHAPTER 4

CONCLUSION

Modal control method of approach is used in this work for designing feedback controllers for a power system in order to improve the dynamic behaviour of the system. Modal controllers are designed with complete state feedback as well as incomplete state feedback, which effectively improve the response of the system. The advantages of the modal control method over the earlier method which uses optimal control theory are discussed.

Some of the possible extensions of the present research are listed below:

(i) The power system model considered in this work is of 8-th order consisting of third order machine, second order exciter-voltage regulator and fourth order prime-mover with speed governor. More detailed dynamics of the machine as well as prime-mover can be included in the model for modal control study.

(ii) In this work the modal control approach is employed to control a single machine power system. The same technique may be applied to control a multimachine power system.

APPENDIX A

For a linear time-invariant system represented by the equation (1)

$$\dot{\underline{x}}(t) = A\,\underline{x}(t) + B\,\underline{u}(t)\ ,$$

let us suppose that the eigenvalues of the open-loop system are distinct. Let $\underline{U}^i$, $\underline{V}^i$, $(i=1,2,\ldots,n)$ are the eigenvectors of matrices A and A' respectively, and diagonal matrix Λ is formed by the n eigenvalues $(\lambda_1, \lambda_2, \ldots, \lambda_n)$ of the system. Then

$$A = U\,\Lambda\,V$$

or

$$V\,A\,U = \Lambda \qquad \text{(A.1)}$$

and

$$\begin{aligned} A\,\underline{U}^i &= \lambda_i\,\underline{U}^i \\ A'\underline{V}^i &= \lambda_i\,\underline{V}^i \qquad (i = 1,2,\ldots,n) \end{aligned} \qquad \text{(A.2)}$$

The two sets of eigenvectors are orthogonal, i.e.,

$$\underline{V}^{i'}\,\underline{U}^j = 0 \qquad (i \neq j;\ \ i,j=1,2,\ldots,n) \qquad \text{(A.3a)}$$

and can be normalised so that

$$\underline{V}^{i'}\,\underline{U}^i = 1 \qquad (i = 1,2,\ldots,n) \qquad \text{(A.3b)}$$

Suppose the first r eigenvalues of the system (1) are shifted using r control variables. Then the first r eigenvectors of A' are to be used as measurement

vectors and the control law is given by

$$u_i = k_i \, \underline{V}^{i'} \, \underline{x} \qquad (i = 1,2,\ldots,r) \qquad (A.4)$$

where k_i's are the controller gains. The closed-loop system is given by

$$\begin{aligned} \dot{\underline{x}}(t) &= (A + B \, \hat{k} \, \hat{V}') \, \underline{x}(t) \\ &= A_1 \, \underline{x}(t) \end{aligned} \qquad (A.5)$$

where $\hat{k}$ is a (rxr) diagonal matrix formed by the controller gains and $\hat{V}$ is the (nxr) matrix given by

$$\hat{V} = [\, \underline{V}^1 \quad \underline{V}^2 \quad \ldots \quad \underline{V}^r \,]$$

In view of eqns. (A.2) and (A.3)

$$\begin{aligned} A_1 \, \underline{U}^i &= A \, \underline{U}^i + B \, \hat{k} \, \hat{V}' \, \underline{U}^i \\ &= \lambda_i \, \underline{U}^i + b_i \, k_i \qquad (i = 1,2,\ldots,r) \\ &= A \, \underline{U}^i \\ &= \lambda_i \, \underline{U}^i \qquad (i = r+1, \, r+2,\ldots,n) \end{aligned} \qquad (A.6)$$

It can be deduced from the eqn.(A.6) that the last (n-r) eigenvalues and eigenvectors of the closed-loop system matrix A_1 are the same as those for the open-loop system matrix A, and only the first r eigenvalues and eigenvectors get modified.

APPENDIX B

MODAL CONTROL METHOD [4,5]

For the linear time-invariant system represented by eqn.(1)

$$\dot{\underline{x}}(t) = A\,\underline{x}(t) + B\,\underline{u}(t)\ ,$$

let us suppose that ℓ of the n eigenvalues either real or complex, or both are to be shifted simultaneously with the restriction that complex eigenvalues occur in conjugate pairs. This can be achieved by using a single control input [4,5]. Let u_1 control input is selected from among the r available control variables (in accordance with the procedure given in Section 2.3). Then the closed-loop system is

$$\dot{\underline{x}}(t) = A\,\underline{x}(t) + b_1\,u_1 \qquad \text{(B.1)}$$

Let ℓ feedback signals are generated from the measurement of all the states using eigenvectors $\underline{V}^i$, $(i = 1,2,\ldots,\ell)$ of A' as measurement vectors and are amplified by ℓ respective controller gains k_i,$(i=1,2,\ldots,\ell)$. Then the control law is given by the sum of these ℓ signals as

$$u_1 = \sum_{i=1}^{\ell} k_i\,\underline{V}^{i'}\,\underline{x} \qquad \text{(B.2)}$$

The closed-loop system is

$$\dot{\underline{x}}(t) = (A + b_1 \sum_{i=1}^{\ell} k_i \underline{V}^{i'}) \underline{x}(t)$$

$$= A_1 \underline{x}(t) \qquad (B.3)$$

In view of the orthoganality conditions of the eigenvectors as given in eqns.(A.3), it follows that

$$A_1 \underline{U}^j = A \underline{U}^j + b_1 \sum_{i=1}^{\ell} k_i \underline{V}^{i'} \underline{U}^j$$

$$= \lambda_j \underline{U}^j \qquad (j=\ell+1, \ell+2, \ldots, n)$$

$$= \lambda_i \underline{U}^i + b_1 k_i \qquad (i= 1,2,\ldots,\ell) \qquad (B.4)$$

From eqn.(B.4) it can be deduced that when ℓ eigenvalues of the uncontrolled system are shifted, the resulting closed-loop system will have ℓ modified eigenvalues and their corresponding eigenvectors and the remaining $(n-\ell)$ eigenvalues and eigenvectors will be unchanged from those of the open-loop system.

In order to calculate the controller gains k_i $(i = 1,2,\ldots,\ell)$, let the new eigenvalues and eigenvectors be ρ_i and $\underline{W}^i$ $(i = 1,2,\ldots, \ell)$. Then

$$A_1 \underline{W}^i = \lambda_i \underline{W}^i \qquad (B.5)$$

Let

$$\underline{W}^i = \sum_{j=1}^{n} q_{ij} \underline{U}^j \qquad (i=1,2,\ldots,\ell) \qquad (B.6)$$

and

$$b_1 = \sum_{j=1}^{n} p_j \underline{U}^j \qquad (B.7)$$

where q_{ij}'s and p_j's are some constants. In view of the eqns.(A.3) and (B.7), the p_j constants are given by

$$p_j = \underline{V}^{j'} \underline{b}_j \quad (j=1,2,\ldots, \ell) \qquad (B.8)$$

Substituting from eqns.(B.3), (B.6) into eqn.(B.5) yields

$$(A + b_1 \sum_{f=1}^{\ell} k_f \underline{V}^{f'}) \sum_{j=1}^{n} q_{ij} \underline{U}^j = \rho_i \sum_{j=1}^{n} q_{ij} \underline{U}^j$$

$$(i=1,2,\ldots,\ell) \qquad (B.9)$$

Since

$$A \underline{U}^j = \lambda_j \underline{U}^j$$

$$A \sum_{j=1}^{n} q_{ij} \underline{U}^j = \sum_{j=1}^{n} q_{ij} \lambda_j \underline{U}^j \quad (i=1,2,\ldots,\ell) \qquad (B.10)$$

Also in view of eqn.(A.3) and (B.8)

$$b_1 \sum_{f=1}^{\ell} k_f \underline{V}^{f'} \sum_{j=1}^{n} q_{ij} \underline{U}^j = b_1 \sum_{f=1}^{\ell} k_f q_{if}$$

$$= \sum_{j=1}^{n} p_j \underline{U}^j \sum_{f=1}^{\ell} k_f q_{if}$$

$$(i=1,2,\ldots,\ell) \qquad (B.11)$$

Making use of eqns.(B.10) and (B.11), eqn.(B.9) can be written as

$$\sum_{j=1}^{n} q_{ij} \lambda_j \underline{U}^j + \sum_{j=1}^{n} p_j \underline{U}^j \sum_{f=1}^{\ell} k_f q_{if} = \rho_i \sum_{j=1}^{n} q_{ij} \underline{U}^j$$

$$(i = 1,2,\ldots,\ell) \qquad (B.12)$$

Eqn.(B.12) is a vector equation in $\underline{U}^j$ and is equivalent to the (nxℓ) scalar equations

$$(\rho_i - \lambda_j)\, q_{ij} - p_j \sum_{f=1}^{\ell} k_f\, q_{if} = 0$$

$$i=1,2,\ldots,\ell \;;\; j = 1,2,\ldots, n \qquad \text{(B.13)}$$

For a given value of i, the first ℓ of these (B.13) equations, i.e., those corresponding to the eigenvalues to be shifted, can be written in the matrix form

$$H_i\, q_i = 0 \qquad \text{(B.14a)}$$

where

$$H_i = [h_{jf}^{(i)}] \qquad \text{(B.14b)}$$

$$h_{jf}^{(i)} = (\rho_i - \lambda_j)\, \delta_{jf} - p_j\, k_f \qquad \text{(B.14c)}$$

$$q_i = [q_{if}] \qquad (i,j,f=1,2,\ldots,\ell) \qquad \text{(B.14d)}$$

and δ_{jf} is the Kronecker delta. Since $q_i \neq 0$ it follows from (B.14a) that

$$|H_i| = 0 \qquad \text{(B.15)}$$

In view of equations (B.14b) and (B.14c), this has the explicit form

$$\begin{vmatrix} (\rho_i-\lambda_1)-p_1k_1 & -p_1k_2 & \cdots & -p_1k_\ell \\ -p_2k_1 & (\rho_i-\lambda_2)-p_2k_2 & \cdots & p_2k_\ell \\ \vdots & \vdots & & \vdots \\ -p_\ell k_1 & -p_\ell k_2 & \cdots & (\rho_i-\lambda_i)-p_\ell k_\ell \end{vmatrix} = 0 \qquad \text{(B.16)}$$

Expansion of the determinant in eqn.(B.16) yields

$$\prod_{j=1}^{\ell} (\rho_i - \lambda_j) = \sum_{f=1}^{\ell} k_f p_f \prod_{\substack{j=1 \\ j\neq f}}^{\ell} (\rho_i - \lambda_j) \quad (i=1,2,\ldots,\ell) \qquad (B.17)$$

which implies

$$\sum_{j=1}^{\ell} \frac{k_j p_j}{(\rho_i - \lambda_j)} = 1 \quad (i=1,2,\ldots,\ell) \qquad (B.18)$$

provided that

$$\rho_i - \lambda_j \neq 0 \quad (i,j = 1,2,\ldots,\ell)$$

Eqn.(B.18) can be solved for k_j to give

$$k_j = \frac{\prod_{f=1}^{\ell} (\rho_f - \lambda_j)}{p_j \prod_{\substack{f=1 \\ f\neq j}}^{\ell} (\lambda_f - \lambda_j)} \quad (j=1,2,\ldots,\ell) \qquad (B.19)$$

which indicates that the controller gains k_j can be realised only when

$$\lambda_i \neq \lambda_j \quad (i,j = 1,2,\ldots,\ell) \qquad (B.20)$$

and

$$p_i \neq 0 \quad (i = 1,2,\ldots,\ell) \qquad (B.21)$$

The inequality in eqn.(B.20) implies that the eigenvalues to be shifted should be distinct and the inequality given by eqn.(B.21) implies that the first ℓ modes of the uncontrolled system should be controllable.

The control law obtained by substituting eqn.(B.19) into eqn.(B.2) has the form

$$u_1 = \sum_{i=1}^{\ell} \left[\frac{\prod_{f=1}^{\ell} (\rho_f - \lambda_i)}{p_i \prod_{\substack{f=1 \\ f\neq i}}^{\ell} (\lambda_f - \lambda_i)} \underline{V}^{i'} \underline{x} \right]$$

$$= \underline{G}' \underline{x} \qquad \text{(B.22)}$$

where $\underline{G}$ is the gain vector the elements of which are given by

$$\underline{G} = \sum_{i=1}^{\ell} \frac{\prod_{f=1}^{\ell} (\rho_f - \lambda_i)}{p_i \prod_{\substack{f=1 \\ f\neq i}}^{\ell} (\lambda_f - \lambda_i)} \underline{V}^{i} \qquad \text{(B.23)}$$

It is to be noted that in case of real systems the control law defined by eqn.(B.22) will be real even in the case of complex eigenvalues. This follows from the fact that if $\lambda_i = \lambda_j^*$, then $\underline{V}^i = \underline{V}^{j*}$ and $p_i = p_j^*$, together with the fact that the required new eigenvalues ρ_i will either occur in conjugate pairs or be real.

APPENDIX C

DESIGN TECHNIQUE FOR INCOMPLETE STATE FEEDBACK CONTROLLER

Let us suppose that ℓ eigenvalues of a linear time-invariant system as represented by eqn.(1)

$$\dot{\underline{x}}(t) = A\,\underline{x}(t) + B\,\underline{u}(t)$$

are to be shifted to preassigned locations with incomplete state feedback using a single control variable, the choice of which is made according to the procedure outlined in section 2.3. Then ℓ measurements of the state variables are to be made using the ℓ corresponding eigenvectors of A' as measurement vectors; and these ℓ signals are given by

$$\eta_i(t) = \underline{V}^{i'}\,\underline{x}(t)$$

$$= v_1^i x_1 + v_2^i x_2 + \ldots + v_n^i x_n \qquad (C.1)$$

$$(i = 1,2,\ldots,\ell)$$

The quantity η_i gives a measure of how much of the i-th mode is present in the system at any instant of time. This follows since if $\underline{x}(t)$ is written in the form

$$\underline{x}(t) = \sum_{i=1}^{n} \alpha_i\,\underline{U}^i \,, \qquad (C.2)$$

then

$$\eta_i(t) = \underline{V}^{i'}\,\underline{x}(t) = \alpha_i \qquad (C.3)$$

It may happen that under normal operating conditions some terms of η_i are much smaller than the others, then these can be omitted from measurement without affecting the value of η_i significantly. With this basis of modal truncation of the modes, the choice of best state variables for incomplete state feedback can be determined[6,7]. The procedure of design is as follows:

Step 1: Determine the ℓ eigenvalues and the corresponding eigenvectors of the transpose of the system matrix.

Step 2: Determine the $\underline{x}^{ss}$ - the average steady state values for the system state vector when the input forcing functions are applied in a step function manner [6]. These values will normally correspond to typical operating values of states, at least when there is no control applied.

$$\underline{x}^{ss} = -\frac{1}{r} A^{-1} \sum_{i=1}^{r} \frac{\underline{b}_i}{\sqrt{\underline{b}_i' \underline{b}_i}} \qquad (C.4)$$

Step 3: Modify the ℓ eigenvectors using the steady state values. The elements of these new eigenvectors are

$$\tilde{v}_j^i = x_j^{ss} v_j^i \qquad (j=1,2,\ldots,n;\ i=1,2,\ldots,\ell) \qquad (C.5)$$

Step 4: Examine each of the new eigenvectors for elements whose absolute value is smaller than that of others by an order of 5 to 10. Select those states for which the corresponding elements of the new eigenvectors are the smallest; and at the same time these states should be

common to all the new eigenvectors. For example, suppose p,q and r elements are the smallest in the first new eigenvector $\underline{V}^1$ and in the subsequent eigenvectors only p and q are the smallest elements, then only p and q states are to be selected.

These state variables selected in the above manner can be omitted from feedback and thus we may achieve incomplete state feedback control of the system. At this stage we may hope for eliminating unmeasurable states as well as some of the measurable states.

Step 5: Obtain the control law assuming complete state feedback using the modal method outlined in Appendix B.

Step 6: Neglect the states as determined in Step 4 from feedback and obtain the controller with incomplete state feedback.

Step 7: Obtain the new steady state values applying this control law and check how close these true steady state values are to the values calculated using the eqn.(C.4). If there is a substantial difference in the relative ratios of various elements of $\underline{X}^{ss}$, then the steps 3 to 6 are to be repeated.

Step 8: Finally obtain the eigenvalues of the resulting closed-loop system with incomplete state feedback and check how the eigenvalues which are not considered for shifting, are affected. In case they are affected to a great extent, then the design may not give satisfactory results.

Step 9: When a number of eigenvalues of the system are to be shifted using different control inputs, this can be done sequentially repeating the above 1 to 8 steps, each time shifting the appropriate eigenvalues with the corresponding choice of control input. However, it should be noted that in this sequential procedure same state variables are to be excluded from feedback at each stage.

APPENDIX D

Nonlinear equations of the power system

The power system considered by Yu et al (1970) is represented by a system of eight nonlinear equations which are given below together with the linearized equations and the numerical values assumed.

Synchronous machine equations

$$\dot{\delta} = w \tag{D.1}$$

$$\dot{w} = \frac{1}{M}(P_i' - D\,w - P_e') \tag{D.2}$$

$$\dot{\psi}_f = v_f - \frac{X_d\ \psi_f}{X_d'\ \tau_{do}'} + \frac{(x_d - x_d')}{X_d'} v_o \cos\delta \tag{D.3}$$

where

$$P_i' \simeq g + 1.5h$$

$$P_e' \simeq \frac{v_o \sin\delta\ \psi_f}{X_d'\ \tau_{do}'} + \frac{(x_d' - x_q)}{2X_d'\ X_q} v_o^2 \sin 2\delta - P_o$$

Exciter-voltage regulator equations

$$\dot{v}_f = -\frac{v_f}{\tau_e} - \frac{\mu_e}{\tau_e}(v_t' + v_s) \tag{D.4}$$

$$\dot{v}_s = -\frac{v_s}{\tau_s} + \frac{\mu_s}{\tau_s} u_1 \tag{D.5}$$

Governor-hydraulic system equations

$$\dot{g} = -\frac{\sigma\ g}{\tau_g} - \frac{1}{\tau_g}\left(\frac{w}{w_o} + g_f\right) \tag{D.6}$$

$$\dot{g}_f = -\frac{g_f}{\tau_a} + \frac{\mu_a}{\tau_a} u_2 \qquad (D.7)$$

$$\dot{h} = \frac{2\sigma g}{\tau_g} + \frac{2}{\tau_g}\left(\frac{w}{w_o} + g_f\right) - \frac{2h}{\tau_w} \qquad (D.8)$$

The nonlinear equations (D.1) to (D.8) of the power system are linearised around an operating point and the real time is scaled for the convenience of computation, which is given by

$$\tau = \beta t \qquad (D.9)$$

where $\beta = 7.308$.

Linearised equations of the power system

The linearised system equations with scaled time are given by

$$\dot{\underline{x}}(\tau) = A\,\underline{x}(\tau) + B\,\underline{u}(\tau) \qquad (D.10)$$

where

$$A = \begin{bmatrix}
0 & 1 & 0 & 0 & 0 & 0 & 0 & 0 \\
a_{21} & \frac{-D}{\beta M} & a_{23} & 0 & 0 & \frac{1}{\beta^2 M} & 0 & \frac{1.5}{\beta^2 M} \\
a_{31} & 0 & a_{33} & \frac{1}{\beta} & 0 & 0 & 0 & 0 \\
a_{41} & 0 & a_{43} & \frac{-1}{\beta\tau_e} & \frac{-\mu_e}{\beta\tau_e} & 0 & 0 & 0 \\
0 & 0 & 0 & 0 & \frac{-1}{\beta\tau_s} & 0 & 0 & 0 \\
0 & \frac{-1}{w_o\tau_g} & 0 & 0 & 0 & \frac{-\sigma}{\beta\tau_g} & \frac{-1}{\beta\tau_g} & 0 \\
0 & 0 & 0 & 0 & 0 & 0 & \frac{-1}{\beta\tau_a} & 0 \\
0 & \frac{2}{w_o\tau_g} & 0 & 0 & 0 & \frac{2\sigma}{\beta\tau_g} & \frac{2}{\beta\tau_g} & \frac{-2}{\beta\tau_w}
\end{bmatrix}$$

$$a_{21} = -\frac{1}{\beta^2 M}\left[\frac{v_o \cos\delta_o \psi_{fo}}{X'_d \tau'_{do}} + \frac{(x'_d - x_q)}{X'_d X_q} v_o^2 \cos 2\delta_o\right]$$

$$a_{23} = -\frac{v_o \sin\delta_o}{\beta^2 M X'_d \tau'_{do}}$$

$$a_{31} = -\frac{(x_d - x'_d) v_o \sin\delta_o}{\beta X'_d}$$

$$a_{33} = -\frac{X_d}{\beta X'_d \tau'_{do}}$$

$$a_{41} = -\frac{\mu_e v_o}{\beta \tau_e v_{to}}\left[\frac{x_q v_{do} \cos\delta_o}{X_q} - \frac{x'_d v_{qo} \sin\delta_o}{X'_d}\right]$$

$$a_{43} = -\frac{\mu_e}{\beta \tau_e v_{to}} \frac{x v_{qo}}{X'_d \tau'_{do}}$$

$$B = \begin{vmatrix} 0 & 0 & 0 & 0 & 1 & 0 & 0 & 0 \\ 0 & 0 & 0 & 0 & 0 & 0 & 1 & 0 \end{vmatrix}'$$

$$\underline{x}(\tau) = [\delta \quad n \quad \psi_f \quad v_f \quad v_s \quad g \quad g_f \quad h]'$$

and

$$\underline{u}(\tau) = [u_v \quad u_g]'$$

where

$$u_v \triangleq \frac{\mu_s u_1}{\beta \tau_s} \quad \text{and} \quad u_g \triangleq \frac{\mu_a u_2}{\beta \tau_a}$$

Besides the other variables are defined by the following equations

$$
\begin{aligned}
X'_d &= (1-xB)\, x'_d + x \\
X_q &= (1-xB)\, x_q + x \\
X_d &= (1-xB)\, x_d + x \\
v'_t &\simeq \frac{v_{do}}{v_{to}}\, v'_d + \frac{v_{qo}}{v_{to}}\, v'_q \\
v'_d &= \frac{x_q\, v_o \cos \delta_o}{X_q}\, \delta \\
v'_q &= \frac{x\, \psi_f}{X'_d \tau'_{do}} - \frac{x'_d\, v_o \sin \delta_o}{X'_d}\, \delta
\end{aligned}
\qquad (D.11)
$$

Further details of the power system are contained in the paper by Yu et al (1970).

Numerical values for different parameters

Transmission line: $x = 0.7417$, $B = 0.1339$

Synchronous machine: $x_d = 1.0$, $x'_d = 0.27$, $x_q = 0.6$

$\tau'_{do}=9.0$, $M=0.02122$, $D = 0.00537$

Exciter-voltage regulator: $\mu_e = 10.0$, $\tau_e = 1.0$, $\tau_s=0.5$

Governor-hydraulic system: $\sigma=0.045$, $\tau_g=0.1$, $\tau_a=0.01$, $\tau_w=1.6$.

μ_a and μ_s values are not needed since they are included in u_g and u_v respectively.

For an initial load and a terminal voltage of the synchronous machine,

$P_o = 0.735$, $Q_o = 0.034$, $v_{to} = 1.05$

the initial currents, voltages, flux linkages and torque angle are

$i_{do} = 0.286$, $i_{qo} = 0.64$, $v_{do} = 0.384$, $v_{qo} = 0.977$,

$v_f = 1.263$, $v_o = 1.058$, $\psi_f = 9.491$, $\delta_o = 0.887$.

REFERENCES

1. Yu, Y.N., Vonsuriya K., and Wedman, L.N., 'Application of an optimal control theory to a power system', IEEE Trans. Power Apparatus and Systems, 1970, Vol. PAS-89, pp. 55-62.

2. Porter B. and Micklethwaite, D.A., 'Design of multi-loop modal control systems', Trans. S.I.T., 1967, Vol. 19, pp. 143-152.

3. Porter B. and Carter, J.D., 'Design of multi-loop modal control systems for plants having complex eigenvalues', Journal of Institute of Measurement and Control, 1968, Vol.1, pp. T61-T68.

4. Porter B. and Crossley, T., 'Synthesis of Aircraft modal control systems having real or complex eigenvalues', A J R Aes., 1969, Vol.73, pp. 138-142.

5. Porter B., Synthesis of Dynamical Systems, 1969, Nelson, London.

6. Davison, E.J. and Goldberg, R.W., 'A design technique for the incomplete state feedback problem', Automatica, 1969, Vol.5, pp. 335-346.

7. Davison, E.J. and Chadha, K.J., 'On the control of a large chemical plant by using modal analysis', Automatica, 1972, Vol.8, pp. 263-273.

8. Grad, J. and Brebner, M.A., 'Eigenvalues and eigenvectors of a general matrix', Comm. ACM, Vol.11, pp. 820-825, 1968.

9. Wonham, W.M., 'On pole assignment in multi-input controllable linear systems', IEEE Trans. Aut. control, 1967, Vol. AC-12, pp. 660-665.

10. Anderson, J.H., 'The control of a synchronous machine using Optimal control theory', Proc. IEEE, 1971, Vol.59, pp. 25-35.

11. Raman, S. and Kapoor, S.C., 'Synthesis of optimal regulator for synchronous machine', Proc. IEE, 1972, Vol.119, pp. 1384-1390.